Hydrogen atom abstraction reactivity of biomimetic distorted dicopper(III) bis(μ-oxo) complexes

Presented in partial fulfillment for the requirements for graduation "With Honors Research Distinction in Chemistry and Biochemistry" in the undergraduate colleges of the Ohio State University

By

Andrew Cypcar

The Ohio State University

November 2019

Project Advisor: Professor Shiyu Zhang, Department of Chemistry and Biochemistry

Introduction

With diminishing liquid petroleum resources, methane has become an important component in supporting our continued need for hydrocarbons and their derived products. Methane is also a potent greenhouse gas, thus its removal from the atmosphere would contribute to reducing global warming. Despite its undesirable greenhouse gas properties, it is continually being produced through biological processes and released into the atmosphere. Additionally, the fossil fuel industry continues to produce a large surplus of natural gas (95% methane)[1] while wastefully burning uncaptured methane with the practice of gas flaring. Despite its abundancy, methane remains an underutilized fuel source due to its low energy density resulting from its gaseous nature. Current strategy to transport methane consists of an energy-intensive cooling and compressing process that converts the gas to liquefied natural gas (LNG) which must be maintained at -162 °C. An alternative strategy is to transport natural gas with pipelines, which are costly to construct and maintain, and not generalizable to remote areas without infrastructure. Methanol, the oxidized analog of methane, can be easily transported in liquid form with trucks, trains, or ships. Therefore, converting methane to methanol would eliminate the need for expensive infrastructure, and wasteful climate change accelerating practices such as flaring would be mitigated if value was added to methane.

The high C-H bond dissociation energy of methane (105 kcal/mol[2]) makes the methane to methanol conversion extremely difficult. Industrially, methane is first converted to syngas (a mixture of CO and H_2) using a process called steam reforming (Scheme 1). This energy-intensive and inefficient method is performed at temperatures of about 750-950 °C and pressures of 20-30 atm.[3] The syngas mixture is then converted to methanol, again at high temperature and pressure.

Scheme 1. Industrial method of methane to methanol conversion.

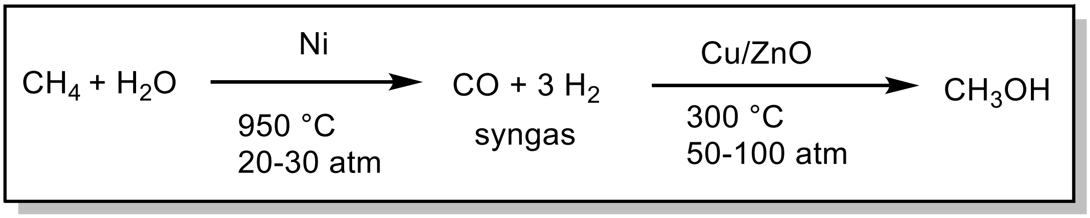

Nature, on the other hand, can perform this difficult reaction with earth-abundant metals at ambient conditions using the enzyme particulate methane monooxygenase (pMMO). pMMO is present in methanotrophic bacteria which convert methane into methanol as their only energy source. Obtaining a clear crystallographic structure of pMMO has been elusive, and a seminal 2010 study postulated pMMO contains a distorted dicopper-oxygen active site (Figure 1).[4]

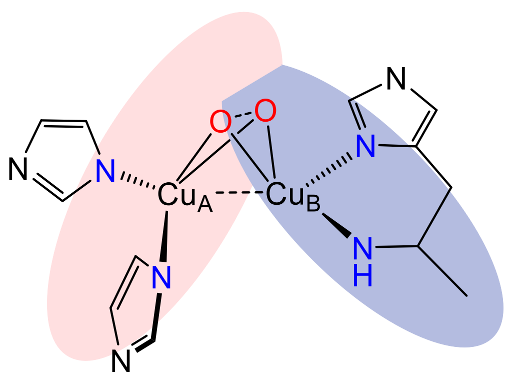

Figure 1. Proposed active site of pMMO.[4]

Since then, the structure of pMMO has been under intense debate. Studies have demonstrated a dicopper site is essential for methane reactivity. EPR[5], UV-vis[6], X-Ray absorption spectroscopy, and theoretical studies[7] corroborate the need for this dicopper-oxygen active site for methane oxidation reactivity. However, recent studies have disputed the original assignment as a dicopper-oxygen center, and now assign the active site as a monocopper center[7,8]. As the debate over the active site continues, the unparalleled and societally important methane reactivity of pMMO lends a prerogative to the study of C-H reactive dicopper-oxygen systems.

Besides pMMO, biological dicopper centers, i.e. coupled binuclear-polyphenol oxidases (CB-PPOs), have been implicated in the oxidative conversion of phenol to quinone moieties. The well-studied CB-PPOs are tyrosinase and catechol oxidase.[9] Tyrosinase catalyzes the oxidation of phenols or catechols to ortho-quinones[10], while catechol oxidases perform only the catechol reaction to ortho-quinones (Scheme 2).

Scheme 2. Oxidation reactions catalyzed by tyrosinase and catechol oxidase.

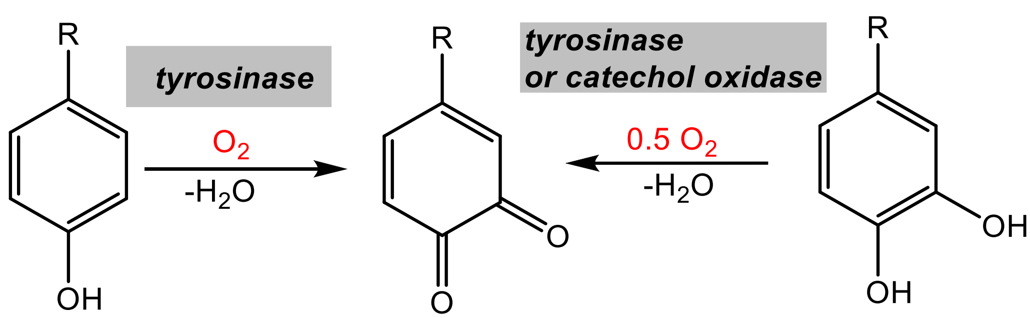

Model system studies have begun to shed light on the mechanism and factors contributing to their oxidative reactivity, yet questions remain regarding the reactive C-H activation intermediate. Through protein crystallography, the dicopper-oxygen active site has been shown to be in the dicopper(II) μ-η^2:η^2-peroxo binding mode in both tyrosinase and catechol oxidases.[10,11] However, model studies have shown an equilibrium exists between the more reactive dicopper(III) bis(μ-oxo) binding mode and the dicopper(II) μ-η^2:η^2-peroxo (Scheme 3), which begs the question as to whether the dicopper(III) bis(μ-oxo) core is the actual active species for C-H oxidation.

Scheme 3. Proposed Binding modes of CB-PPOs.[4]

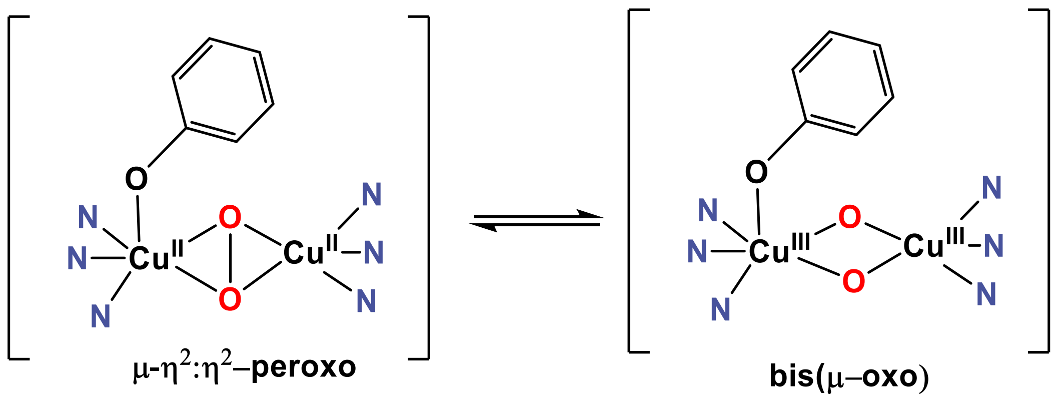

Additionally, model studies[4] have not achieved the reaction rates present in enzymes, suggesting the existence of unknown factors that contribute to the high oxidative reactivity of the dicopper active sites. Understanding the structure and mechanisms of the active dicopper-oxygen moiety could open new possibilities to rationally design biomimetic catalysts for industrially relevant C-H oxidation reactions.

Focus of this Study

An understudied component of dicopper-oxygen model systems is the degree of distortion of the core. The previously postulated dicopper active site of pMMO shows a distorted, asymmetric coordination feature, namely a 67° torsion angle between the copper atoms. The two copper atoms are ligated by different nitrogen donors, which would also contribute to an asymmetrical electronic environment. In another example of distortion, a recent crystal structure of a catechol oxidase shows a butterfly distortion (Figure 2) and an O-O distance of 1.9 Å[11], which is between the preferred length for a dicopper(III) bis(μ-oxo) (2.34 Å) and dicopper(II) μ-η^2:η^2-peroxo (1.45 Å).[9] Moreover, a recent crystal structure of tyrosinase also shows the dicopper(II) μ-η^2:η^2-peroxo active site in the bridged-butterfly conformation.[10]

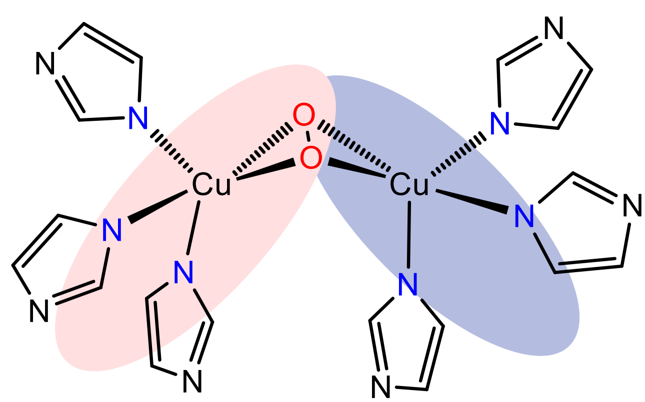

Figure 2. Structure of active site of catechol oxidase[11] (PDB: 4Z13).

Although the active site of tyrosinase was assigned as dicopper(II) μ-η^2:η^2-peroxo, the authors conclude the interconversion to the dicopper(III) bis(μ-oxo) form could not be ruled out with the UV-vis and Raman data they collected.[10] Multiple studies have also shown the active site of tyrosinase to be "flexible".[10,12] Perhaps this flexibility is needed to adapt the active site to a more distorted and favorable reactive intermediate. Together, these studies clearly show distortion of the active site is a common feature in highly C-H reactive dicopper-oxygen enzymes.

Considering the electronic structure, asymmetry of the active site leads to differing orbital overlap compared to a planar analog. In comparison to asymmetric dicopper-oxygen active sites, it is useful to examine hemocyanin, a dicopper enzyme that contains a planar core (Figure 3). Despite apparent similarities to pMMO and CB-PPOs, Hemocyanin does not react with sp^3 C-H bonds.

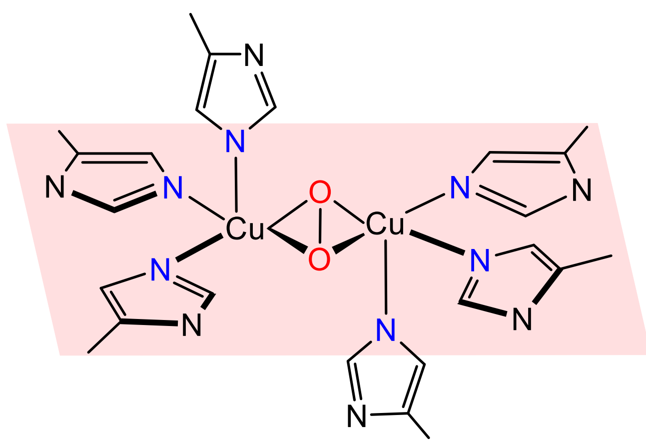

Figure 3. structure of hemocyanin oxygen binding site (PDB: 1JS8).

The arrangement of the dx^2-dy^2 orbitals in a planar dicopper-oxygen core maximizes superexchange, affording strong anti-ferromagnetic coupling between ligands. Anti-ferromagnetic coupling results in an S = 0 singlet state, which is a closed shell species that is not potent towards homolytic C-H bond scission. Therefore, the planar hemocyanin has no oxidative reactivity towards C-H bonds. A distorted environment would disrupt the anti-ferromagnetic coupling between the two copper centers by reducing the overlap between dx^2-y^2 orbitals and thus lowering the singlet to triplet energy gap. Interestingly, theoretical calculations show the S = 1 triplet state of dicopper-oxo species have higher H atom transfer reactivity, which implores us to explore if a distorted dicopper oxo core can have enhanced reactivity comparing to its symmetric counterpart (Scheme 4).

Scheme 4. Influence of geometric distortion on the electronic character of dicopper(III)-oxygen site.

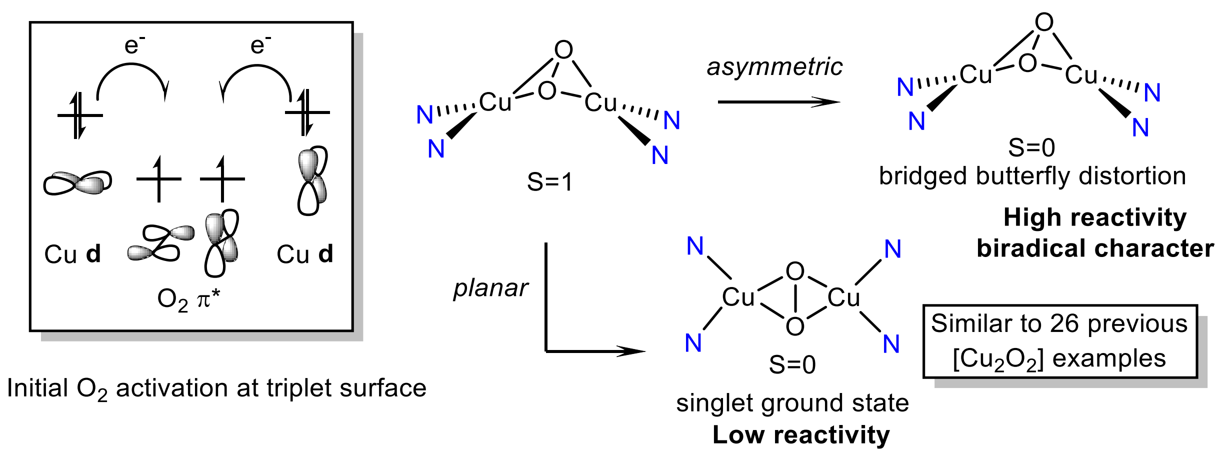

By mimicking these dicopper enzymes structure and functionality, we believe unsymmetrical bimetallic catalysts show promise in converting methane to methanol at ambient pressures and temperatures. Ideally, our proposed unsymmetrical dicopper catalyst would follow the below mechanism of hydrocarbon oxidation (Scheme 5). The H-atom abstraction (HAA) step is the focus of this thesis, and future studies will examine the radical recapture abilities of the dicopper complex.

Scheme 5. Proposed mechanism for hydrocarbon oxidation by a dicopper-oxo catalyst.

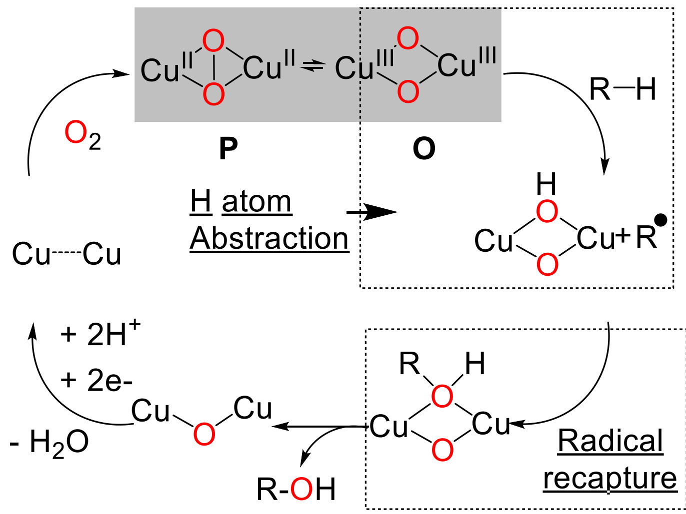

Rational Design of Distorted Dicopper-oxo Complexes

Many models and systems have been explored to mimic dicopper-oxo active sites of both pMMO[9] and tyrosinase[9], yet none have specifically examined the effect of the distortion feature on reactivity. The copper-oxygen mode is well-studied, and the most reactive moiety is thought to be a dicopper(III) bis(μ-oxo).[15] Aligned with these studies, we aimed to prepare a dicopper(III) bis(μ-oxo) species with a new focus on creating distorted moieties. Our model creates distortion in the core through ligand design. In fidelity to the enzyme active sites, we used nitrogen-donor ligands. Generally, it is necessary to use sterically bulky ligands in order to form dicopper-oxygen cores. To create asymmetrically distorted $[Cu_2O_2]^{2+}$ moieties, we used particularly bulky C_2 symmetric bidentate bis(oxazoline) ligands. The work of Meyer and coworkers[13] demonstrates how dicopper(III) bis(μ-oxo) cores can be prepared from these ligands. The advantage of using bis(oxazoline) ligands is that the R-group can be easily changed, which in turn allows for tuning of the electronic and steric environment (Figure 4). To see if the distortion alone is the cause of reactivity, two models with differing degrees of distortion were prepared in this study, synthesized from two bis(oxazoline) ligated Cu(I) complexes.

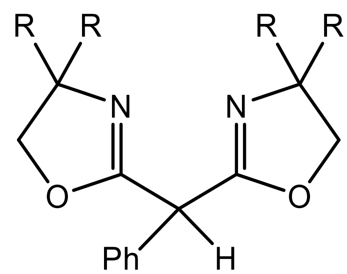

General BOX structure

Figure 4. General structure of bis(oxazoline) ligands. The arm R groups can be easily modified to tune the degree of asymmetry.

Results and Discussion

To create a dicopper-oxo complex that is twisted with respect to the copper centers, the bis(oxazoline) $^{Ph,H}BOX_{Me2}$ ligand (1,1-bis(4,4-dimethyl-1,3-oxazolin-2-yl)-1-phenylmethane) was used (Figure 5).

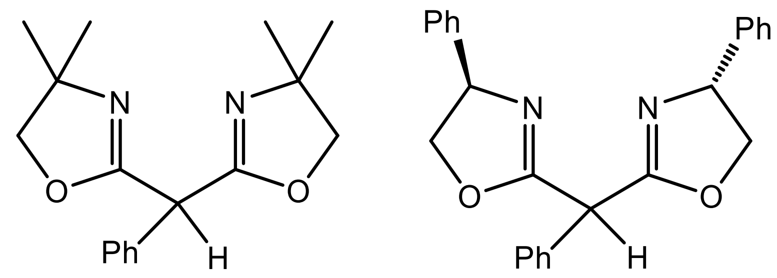

Figure 5. Structure of bis(oxazoline) ligands $^{Ph,H}BOX_{Me2}$ (left) and $^{Ph,H}BOX_{Ph,H}$ (right).

Treatment of this ligand with 1 equiv of $[Cu^{I}(MeCN)_4]PF_6$ affords a white powder with ^{1}H NMR signals expected of $[(^{Ph,H}BOX_{Me2})Cu^{I}]PF_6$. This complex can be stored at -40 °C without decomposition for approximately two months. In order to stabilize the desired electropositive Cu(III) oxidation state, the weakly acidic H atom in the backbone of the ligand was deprotonated with the addition of 1 equiv of $LiO^{t}Bu$. This treatment affords $[(^{Ph}BOX_{Me2})Cu^{I}(MeCN)]$ in 48% yield, and the ^{1}H NMR signal shows an additional peak corresponding to the neutral ligand MeCN and disappearance of the singlet peak corresponding to the H atom in the backbone. Treatment of $[(^{Ph}BOX_{Me2)}Cu^{I}(MeCN)]$ with O_2 at -80 °C in THF resulted in the formation of a dark purple complex (further denoted **O**-Me$_2$). UV-vis spectroscopic features suggest the dicopper(III) bis(μ-oxo) binding mode is afforded, evidenced by the bands formed at 337 nm and 399 nm (Figure 6). These features are stable in the UV-vis at -80 °C for greater than 3 hours, but decay slowly when warmed to -70 °C. A beers law plot was used to determine that the molar absorptivity of the 337 nm peak is 12,000 $M^{-1}cm^{-1}$. No interconversion to the dicopper(II) μ-η^2:η^2-peroxo core is observed for this compound.

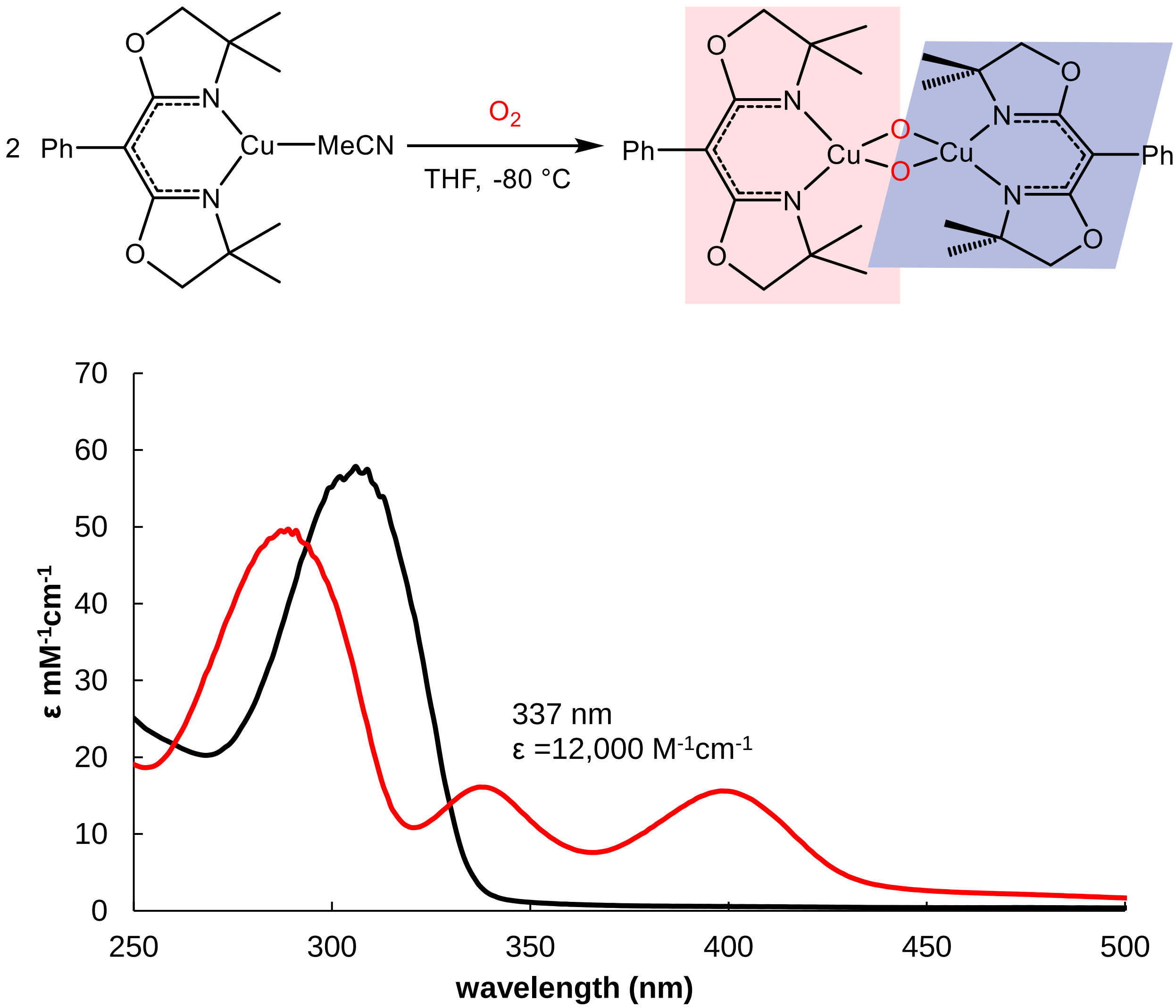

Figure 6. Reaction scheme (top) and corresponding UV-Vis spectra (bottom) (-80 °C, 0.05 mM **O**-Me$_2$,THF) The black line is the spectrum before oxygen is added, and the red line is the spectrum after oxygen is added.

To create an even more distorted $[Cu_2O_2]^{2+}$ entity, the bis(oxalzine) $^{Ph,H}BOX_{Ph,H}$ ligand (1,1-Bis(4,4-diphenyl-1,3-oxazolin-2-yl)-1-phenylmethane) was used (Figure 5). Treatment of the ligand with 1 equiv of CuO^{t}Bu, which simultaneously metallates the ligand and deprotonates the backbone, affords a tan colored powder in 94% yield with ^{1}H

NMR signals expected of [(^{Ph}BOX$_{Ph,H}$)Cu^{I}(MeCN)]. This compound is also stable at -40 °C for approximately 2 months. Treatment of [(^{Ph}BOX$_{Ph,H}$)Cu^{I}(MeCN)] with O_2 at -80 °C in THF resulted in the formation of a dark purple complex (further denoted **O**-Ph,H). UV-vis spectroscopic features suggest the dicopper(III) bis(μ-oxo) binding mode is afforded, evidenced by the shoulder formed at 311 nm and the band formed at 364 nm (Figure 7). These features are stable in the UV-vis at -80 °C for greater than 3 hours, but decay slowly when warmed to -70 °C. A beers law plot was used to determine that the molar absorptivity of the 365 nm peak is 17,500 $M^{-1}cm^{-1}$. No interconversion to the dicopper(II) μ-η^2:η^2-peroxo core is observed for this compound.

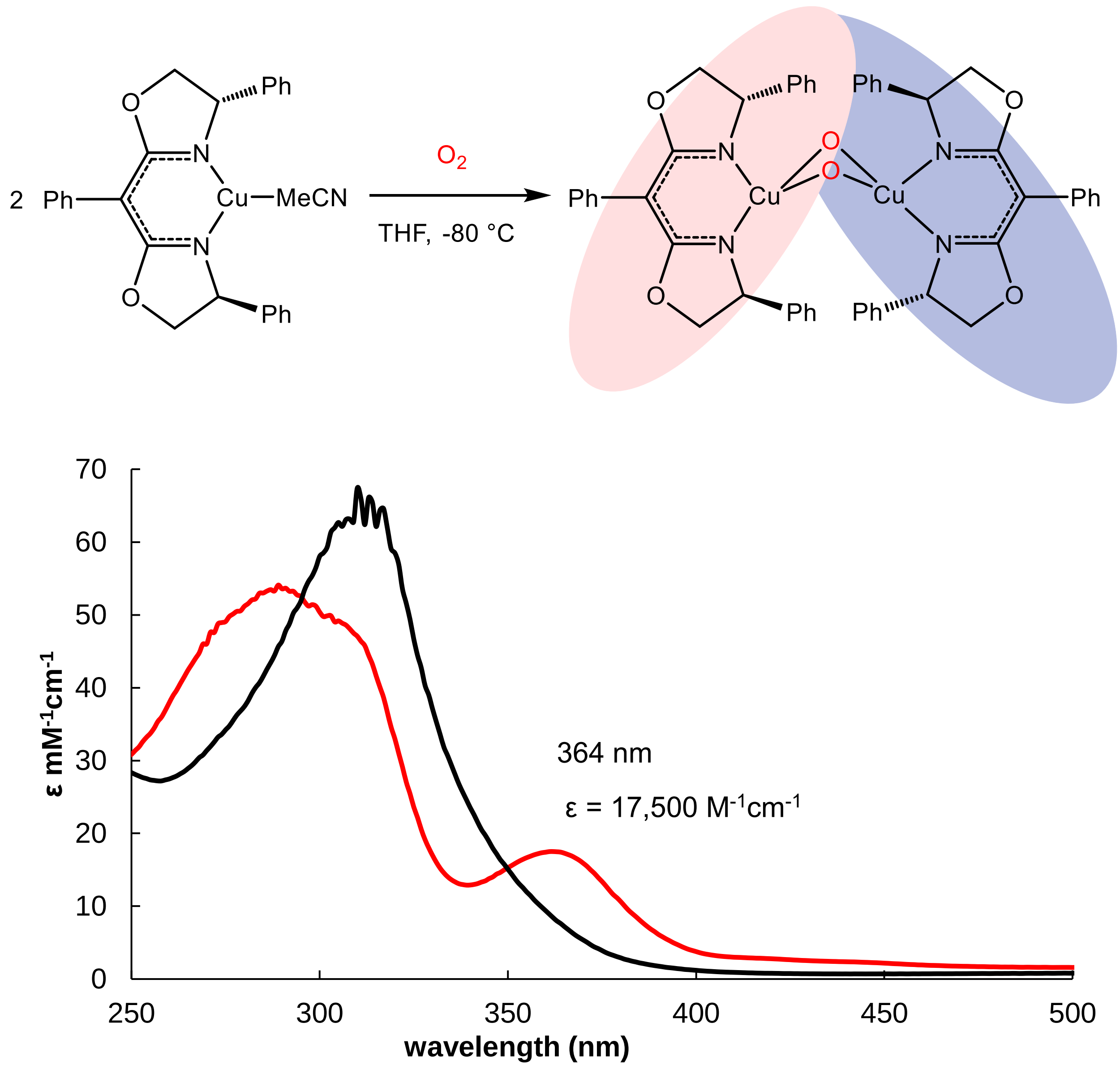

Figure 7. Reaction scheme (top) and corresponding UV-Vis spectra (bottom) spectra -80 °C , 0.05 mM **O**-Ph,H, THF). The black line is the spectra before oxygen is added, and the red line is the spectra after oxygen is added.

Predicted Geometric Distortion of Synthesized $[Cu_2O_2]^{2+}$ Compounds

We were delighted to find that both copper complexes were able to form the desired bis(μ-oxo) cores. Their temperature stability is also consistent with previous studies, as most bis(μ-oxo) complexes are not stable below -80 °C. With two complexes to compare, we began to evaluate the geometric environment and distortion of the two cores. A previous study creates $[Cu_2O_2]^{2+}$ entities using very analogous $[(^{Me,H}BOX_{Me2})Cu^{I}]PF_6$ complexes, so we are confident in assigning the structure of our $^{Ph}BOX_{Me2}$ ligated complex based on their UV-Vis features. The crystal structure obtained for the $[(^{Me,H}BOX_{Me2})_2Cu_2O_2]^{2+}$ compound shows a 48 degree twist from planarity.[13] We also performed DFT geometry optimization calculations for the $^{Ph,H}BOX_{Me2}$ ligated complex and a 34 degree torsion angle was predicted. This information supports the assignment of **O**-Me_2 as having a twisted core.

There is little literature precedence for what type of distortion **O**-Ph,H could adopt. After failing to obtain a crystal structure at -80 °C for **O**-Ph,H, we turned to DFT to compute lowest energy arrangements for the compound. These calculations show a modest 6.7 degree twist from planarity with the oxo ligand above the plane of the coppers in a bridged-butterfly configuration. The hydrogen atoms attached at the same carbons as the phenyl rings show favorable σ-π interactions with the phenyl rings on the opposing complexes. The directionality of this interaction biases the bridged-butterfly core distortion. There is some precedence for this structure: crystal structures have been obtained for dicopper(II) μ-η^2:η^2-peroxo dicopper-oxo complexes in the bridged butterfly conformation.[14,15] Although in the dicopper(II) μ-η^2:η^2-peroxo binding mode, these structures lend support to the possibility that the similar dicopper(III) bis(μ-oxo) core could have a bridged-butterfly distortion. Further calculations of **O**-Ph,H support that the reactive triplet state of oxygen would be retained in this geometry. If this core is indeed the structure of **O**-Ph,H, the reactivity of the bridged-butterfly compound could have exciting relevance to tyrosinase and CB-PPOs. Resonance Raman studies need to be carried out to definitively assign the binding mode of both **O**-Ph,H and **O**-Me_2 compounds. In addition, more structural studies should be pursued in the future, and unequivocal assignment through crystallography of **O**-Ph,H having a "bridged butterfly" core would be extremely significant. Using the information that has been obtained, **O**-Me_2 will be further assigned in this work as having "twisted" distortion and **O**-Ph,H will be best assigned as having a bridged-butterfly distortion (Figure 8).

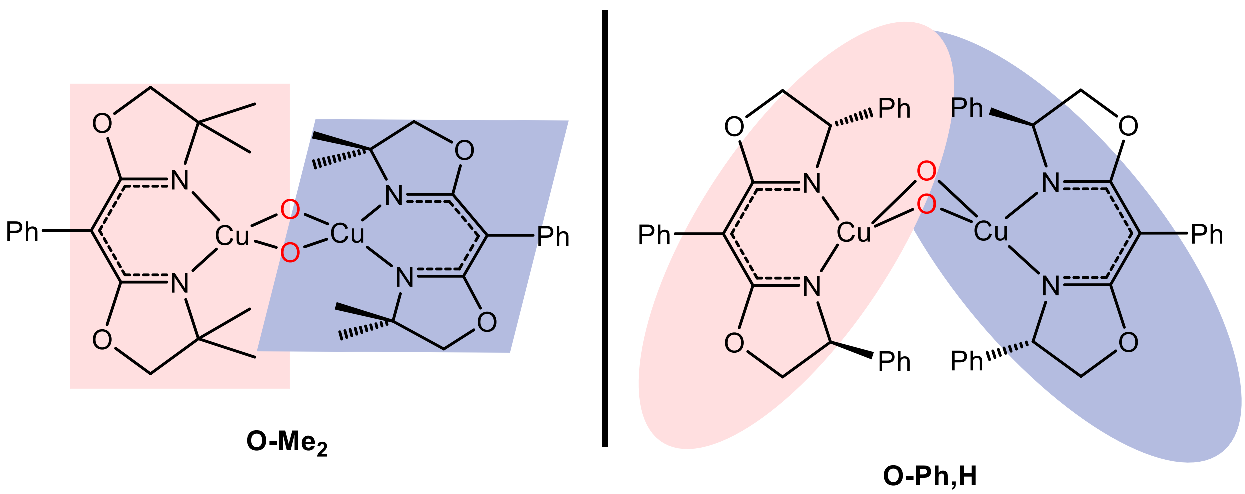

Figure 8. Assigned geometric structures of **O**-Me_2 (left) and **O**-Ph,H (right).

Although reactivity studies with planar dicopper(III) bis(μ-oxo) complexes are numerous, ligand effects can have a huge influence on reactivity. For this reason, a planar analog of **O**-Ph,H and **O**-Me_2 using bis(oxazoline) ligands should be synthesized.

Synthesis of this planar analog was attempted using two different ligands, $^{Ph,H}BOX_{H,H}$ and $^{Ph,H}BOX_{Me,H}$. In contrast to **O**-Ph,H and **O**-Me_2 these ligands are less sterically bulky, which should lead to a core with no geometric distortion. Unfortunately, the corresponding Cu(I) complexes could not be synthesized with a variety of solvents, even at low temperatures. We speculate a fast disproportionation of the Cu(I) complexes to Cu(II) and Cu(0). To work around this problem, UV-vis studies were carried out at lower temperatures to see if these ligands could form a dicopper(III) bis(μ-oxo) in-situ. Unfortunately, these in-situ studies did not yield the desired dicopper(III) bis(μ-oxo) cores, and there was appearance of 1 band at 520 nm when $^{Ph,H}BOX_{Me,H}$ is used (Figure S3) and 1 band at 500 nm when $^{Ph,H}BOX_{H,H}$ is used (Figure S4). These bands likely correspond to homolyptic $[(^{Ph,H}BOX_{H,H})_2Cu^{II}]^{2+}$ and $[(^{Ph,H}BOX_{Me,H})_2Cu^{II}]^{2+}$ tetrahedral complexes.

We were inspired by the work of Stack and coworkers[16,17], where they demonstrated how nitrogen-based ligands can “capture” a pre-made bis(μ-oxo) core in at low-temperature through ligand exchange. We attempted to synthesize a $[Cu_2O_2]^{2+}$ core by adding $^{Ph,H}BOX_{Me,H}$ to a pre-made dicopper(III) bis(μ-oxo) species (Scheme 6). This core was prepared at -80 °C using N,N,N′,N′-tetramethyl-1,3-propanediamine (TMPD) ligands and the $[Cu^I(MeCN)_4]CF_3SO_3$ salt. After the core was formed, it was subsequently treated with $^{Ph}BOX_{Me,H}$ to see if the ligand would “capture” the pre-made core by displacing the TMPD ligands.

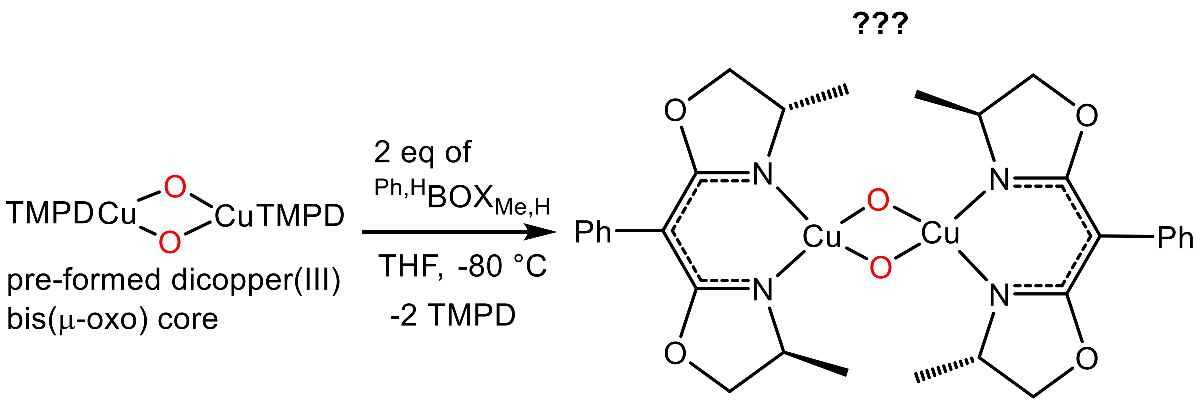

Scheme 6. Summary of core capture. A pre-formed bis(μ-oxo) core was formed and was treated with $^{Ph}BOX_{Me,H}$ in an attempt to displace the TMPD ligands while retaining the $[Cu_2O_2]^{2+}$ structure.

Unfortunately, no new peaks are present after adding the BOX ligand. Warming the reaction mixture from -80 °C to -60 °C affords a new compound with a 520 nm peak attributed to the disproportionated products (Figure S5). This same core-capture procedure was attempted with $^{Ph}BOX_{H,H}$, and again the disproportionation product is formed.

Despite trying two ligands, in-situ synthesis, and core-capture methods, a planar analog of **O**-Ph,H and **O**-Me_2 could not be obtained. However, there is still likely differing degrees of distortion between the **O**-Ph,H and **O**-Me_2 cores, and therefore reactivity differences can be compared and attributed to differing degrees of distortion.

HAA Reactivity Studies of O-Ph,H and O-Me_2

The HAA reactivity difference between **O**-Ph,H and **O**-Me_2 was first compared with a hydrogen atom donor with a weak O-H bond, i.e. TEMPO-H (BDE = 70 kcal/mol).[2]

TEMPO-H is a common hydrogen atom donor substrate and is considered one of the easiest targets for HAA. When treated with 1 eq of TEMPO-H, the dicopper(III) bis(μ-oxo) bands of **O**-Ph,H and **O**-Me_2 decrease rapidly, indicating a fast reaction. The absorbance of the 337 nm peak of **O**-Me_2 and 365 nm peak of **O**-Ph,H was monitored over time to obtain the reaction rate. **O**-Ph,H reacted a considerable 14 times faster than the **O**-Me_2 compound (Figure 9).

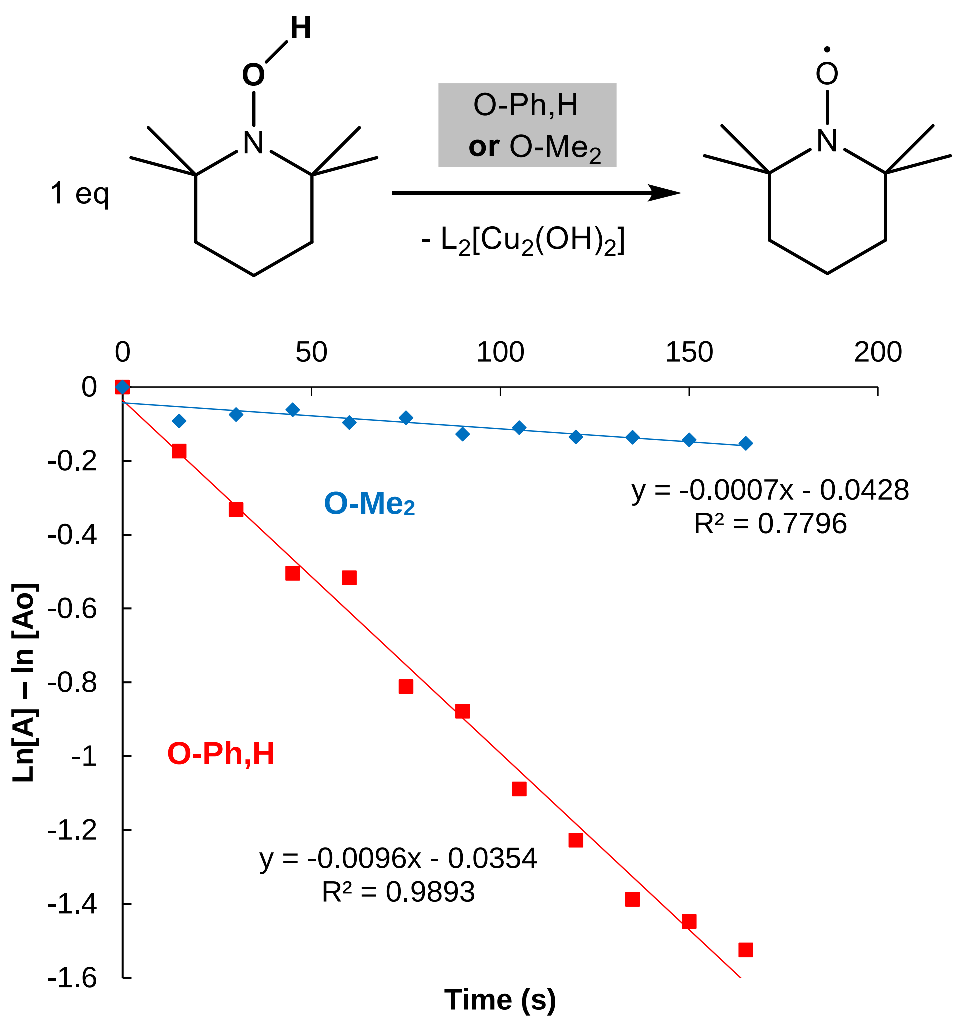

Figure 9. Reaction scheme (top) and pseudo first order decay plot (bottom). The **O**-Ph,H reactivity (red line) was compared to **O**-Me_2 reactivity (blue line) for TEMPO-H.

Although TEMPO-H has a weak bond dissociation energy, this exciting result demonstrates there is a significant reactivity difference between the two models. To further demonstrate reactivity differences, stronger C-H bond substrates were tested. C-H bond substrates are also clearly better analogs to methane, and O-H bond dissociation reactions have been demonstrated to be affected by proton-coupled electron transfer, making their kinetic analysis more convoluted. When treated with 100 equivalents of the common C-H substrate 9,10-dihydroanthracene (DHA) (BDE = 76 kcal/mol[2]), **O**-Ph,H reacts slowly over 1 hour with a second order rate of $k = -0.02\ M^{-1}s^{-1}$. Over the same time period, **O**-Me_2 was barely consumed at the same condition, $k = -8.8 \times 10^{-4}\ M^{-1}s^{-1}$. Overall, **O**-Ph,H reacts 22 times faster than **O**-Me_2 for this substrate (Figure 10).

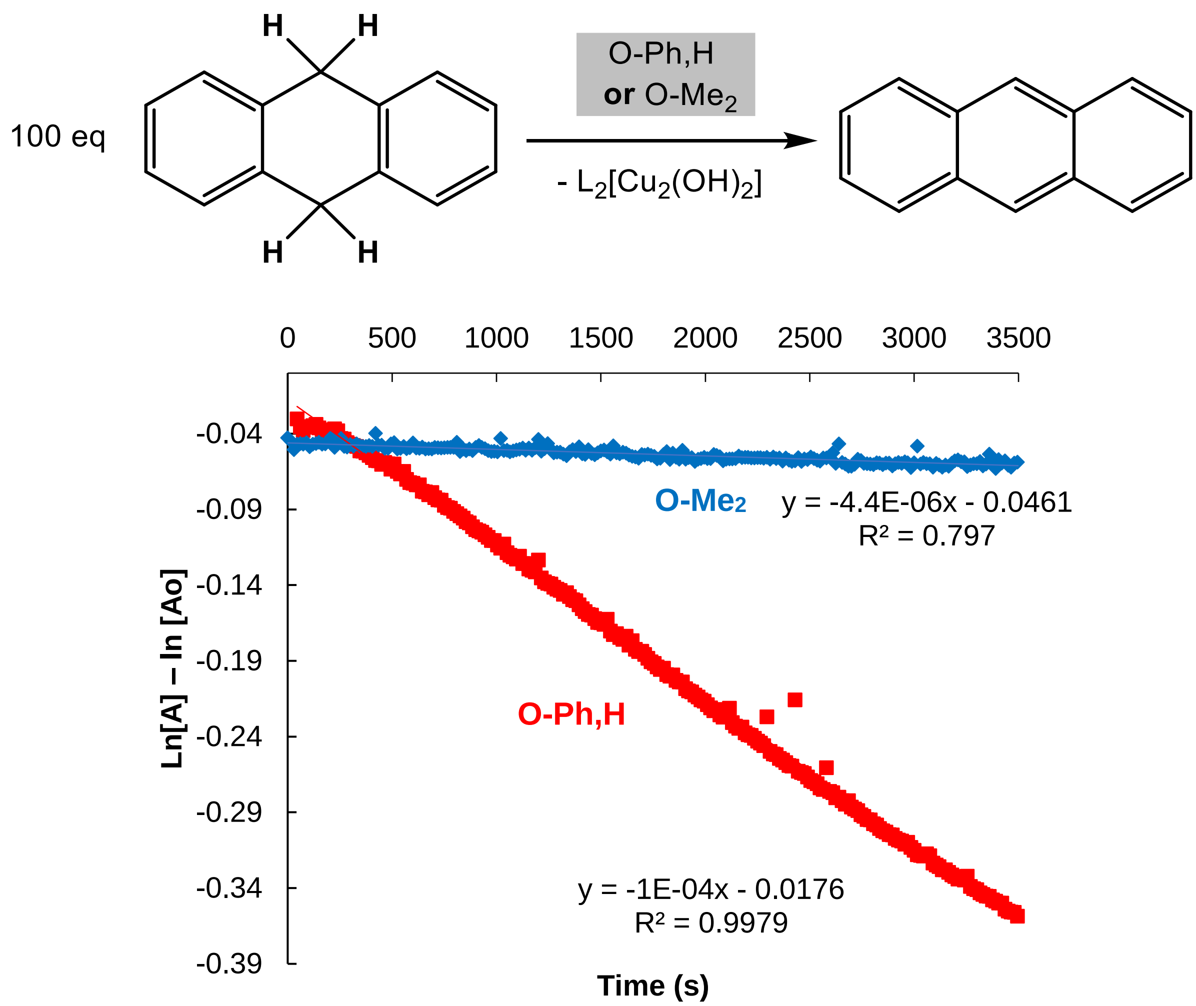

Figure 10. Reaction scheme (top) and pseudo first order decay plot (bottom). The **O**-Ph,H reactivity (red line) was compared to **O**-Me2 reactivity (blue line) for 9,10-dihydroanthracene.

In order to study how steric bulk affects the reaction rate a smaller C-H substrate 1,4-cyclohexadiene (BDE = 77 kcal/mol[2]) was used. It is significantly less sterically bulky than DHA, and thus may have easier access to the $[Cu_2O_2]^{2+}$ cores. When treated with 1000 equivalents a 300 times enhancement of the reaction rate of **O**-Ph,H (k = -0.014 $M^{-1}s^{-1}$) versus **O**-Me2 (k = -4.6×10^{-5} $M^{-1}s^{-1}$) is observed (Figure 11).

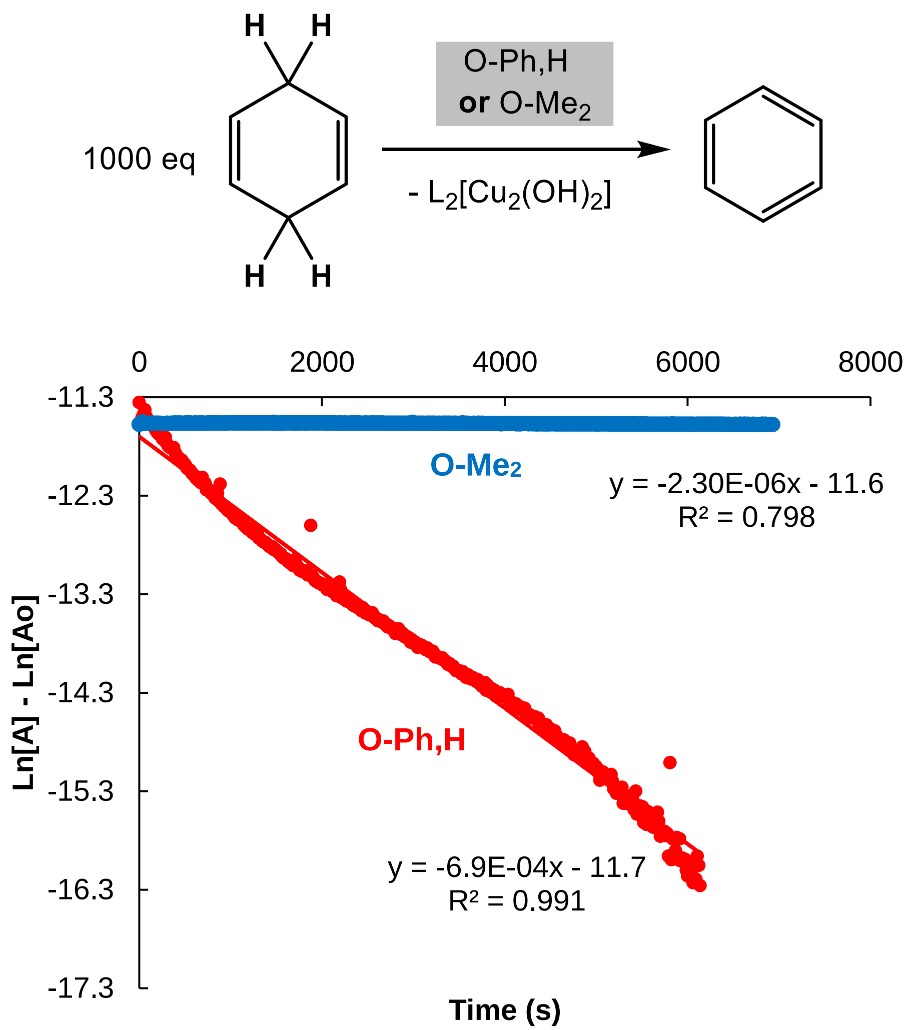

Figure 11. Reaction scheme (top) and pseudo first order decay plot (bottom). The **O**-Ph,H reactivity (red line) was compared to **O**-Me_2 reactivity (blue line) for 1,4-cyclohexadiene.

The bond dissociation energies of 1,4-cyclohexadiene and DHA are nearly the same, yet there is a substantial reactivity difference-- this suggests steric factors may be contributing to the reaction speed. 1,4-cyclohexadiene is a smaller molecule than DHA, so it would be affected more if the $[Cu_2O_2]^{2+}$ core is difficult to access sterically. This suggests geometric structure in our two models: the 1,4-cyclohexadiene is sterically small enough to access the core of **O**-Ph,H, but too large to access the core of **O**-Me_2. DHA is nearly too large for both models, so there is a more modest rate difference. A summary of the 2nd order reaction rates of the two complexes with three substrates is shown in table 1.

Table 1. Summary of 2nd order reaction rates between $[Cu_2O_2]^{2+}$ compounds.

Substrates	**O**-Ph,H rate ($M^{-1}s^{-1}$) (butterfly distortion)	**O**-Me_2 rate ($M^{-1}s^{-1}$) (Twisted distortion)	Rate ratio **O**-Ph,H / **O**-Me_2
9,10-DHA	-0.02	-8.8 x 10^{-4}	22
1,4-cyclohexadiene	-0.014	-4.6 x 10^{-5}	300
TEMPO-H	-190	-14	14

In order to compare the HAA reactivity of the potent **O**-Ph,H to literature model complexes a more accurate 2nd order rate constant was determined. Under pseudo-first order conditions, different concentrations of 1,4-cyclohexadiene were added to **O**-Ph,H. The decay of the 364 nm peak was monitored, and the natural log of the concentration was plotted against the time of the reaction. The observed rate, $k_{obs,}$ was then plotted against each respective concentration used (Figure 12). The slope of the line multiplied by the concentration of **O**-Ph,H is the rate constant. This more accurate 2nd order rate constant was determined to be -0.006 $M^{-1}s^{-1}$ at -80 °C.

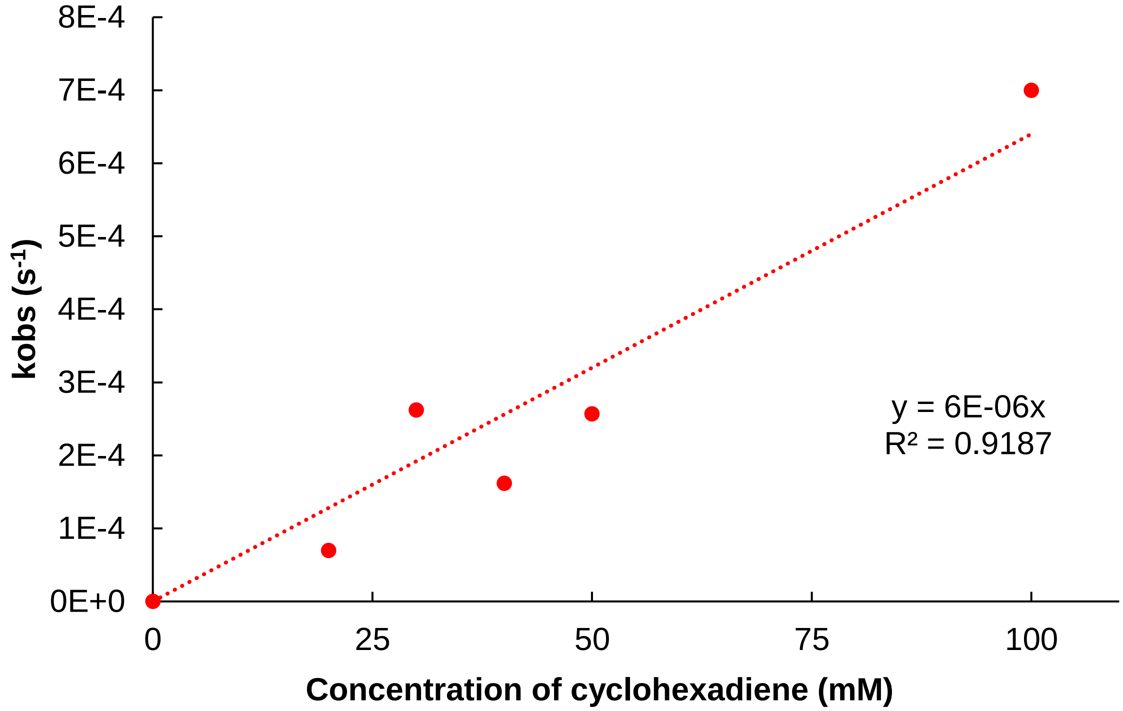

Figure 12. First order dependence of decay of **O**-Ph,H with 1,4-cyclohexadiene at -80 °C, used to obtain a more accurate second order rate constant.

The 2nd order rate constant in a similar study[17] of a particularly reactive $[(TMPD)_2Cu_2O_2]^{2+}$ moiety treated with 9,10-DHA was -0.07 $M^{-1}s^{-1}$ at -125 °C, 12 times faster than **O**-Ph,H at -80 °C. Although **O**-Ph,H is less reactive, the ligand used in the similar study is much less sterically bulky, and substrate access to the core may explain the enhanced reactivity. Future experimental and computational studies should examine the effect of substrate size on the reaction rate and the energy of the transition state. This reactivity comparison also further supports the assignment of **O**-Ph,H as having a dicopper(III) bis(μ-oxo) core, as dicopper(II) μ-η^2:η^2-peroxo cores are much less reactive.

End Products Analysis

To characterize the end products of the reaction, we turned to electron paramagnetic resonance (EPR). The O-H donor 2,4-ditertbutyl phenol (BDE = 86 kcal/mol[2]) was used as a substrate because it reacts fully with **O**-Ph,H in approximately 1.5 hr with 100 equivalents. The C-H donors react more slowly, and we wanted to guarantee the core was fully reacted before taking the measurement. Following treatment of **O**-Ph,H with 100 eq of 2,4-ditertbutyl phenol, the following spectrum was obtained (Figure 13). The 4 peaks correspond to a four-line axial Cu(II) signal, so the reaction of **O**-Ph,H with an H-atom substrate results in a Cu(II) species.

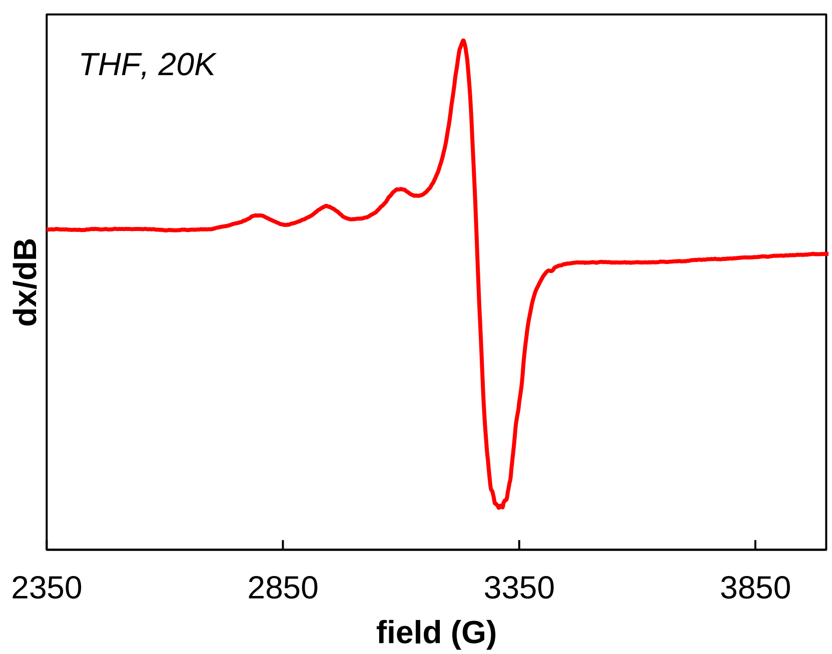

Figure 13. EPR spectrum of **O**-Ph,H treated with 100 eq of 2,4-ditertbutylphenol (THF, 20 K, 0.1 mM [Cu_2]).

Along with EPR, analysis of the UV-vis spectrum following the reaction of **O**-Ph,H with 1,4-cyclohexadiene and 9,10-DHA lends further insight into the end product of the reaction. After **O**-Ph,H completely reacts with either of these substrates, a UV-vis spectrum with multiple weak features is observed (Figure 14).

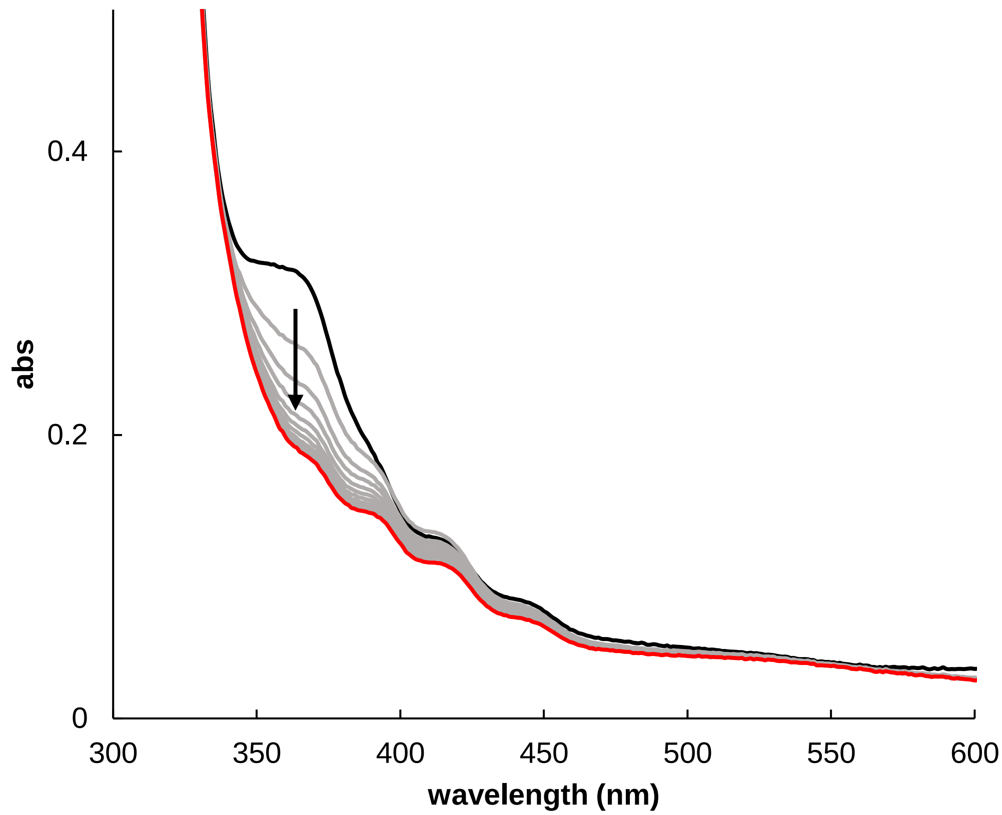

Figure 14. UV-Vis spectrum showing decay of **O**-Ph,H peak after treatment of 1,4-cyclohexadiene. The feature is fully decayed (red line) after 2 hr, yielding a spectrum with multiple weak peaks.

When warmed to -70 °C, the features of this ending spectrum decay further leaving no observable UV-vis bands. Since these features decay at temperatures greater than

-70 °C, the end product could be a temperature-sensitive copper-oxygen species. Taking these observations into account and considering the EPR data specifically shows a Cu(II) species, we propose the following mechanism to explain the formation of a temperature sensitive Cu(II)-oxygen species from the HAA reaction of O-Ph,H with H atom substrates (Scheme 7).

Scheme 7. Proposed mechanism of HAA with **O**-Ph,H.

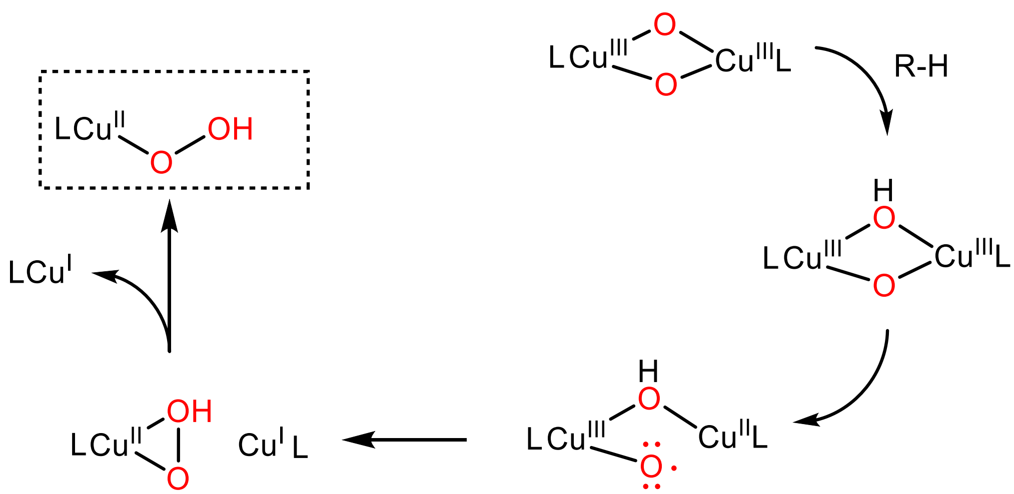

The end product, Cu(II) hydroperoxo, is characterized in the literature. Examples of copper(II) hydroperoxo species typically have a peak of 320-380 nm, with molar absorptivity values ranging from 700 $M^{-1}cm^{-1}$ to 5000 $M^{-1}cm^{-1}$, and a four-line axial Cu(II) EPR signal.[9] The fully reacted UV-vis spectrum of **O**-Ph,H does have a peak at 370 nm along with several other peaks. The other small UV-vis features could be attributed to a tricopper-oxygen species, but further characterization with crystallography and resonance Raman should be carried out to fully determine the end product. Knowing the identity of the end product would contribute to our mechanistic understanding of the **O**-Ph,H system.

The end product of **O**-Me_2 is more easily characterized. After **O**-Me_2 fully reacts with substrates, a weak broad band forms at 700-800 nm which likely corresponds to a dicopper(II) bis(μ-hydroxo) species (typically have broad 600-700 nm feature[22]). This would be consistent with the prediction that **O**-Me_2 is abstracting an H atom from the substrates, however it is not regenerating the catalyst through a radical rebound step.

Conclusions

Two novel $[Cu_2O_2]^{2+}$ model compounds with different degrees of distortion were synthesized and a reactivity difference between the two was demonstrated. **O**-Ph,H, best assigned as having a bridged-butterfly geometric distortion, proved to be 10-300 times more reactive than the twisted **O**-Me_2 species towards C-H and O-H substrates. The more potent **O**-Ph,H species was further explored with kinetic, mechanistic, and end product analyses. The second-order rate constant for the reaction **O**-Ph,H and 9,10-DHA was obtained, and found to be similar to existing dicopper(III) bis(μ-oxo) dicopper-oxo models. EPR and UV-Vis data suggest a Cu(II) end product is formed, but more thorough analysis needs to be carried out to unequivocally determine the ending product. Although the degree and type of distortion of **O**-Ph,H was not unambiguously determined in this study, a stark reactivity difference is observed with these two compounds with structures electronically similar yet different in steric bulk. The preliminary knowledge gained from this study—that distortion can increase reactivity—can be applied to current thinking about tyrosinase and pMMO function, among other dicopper-oxygen enzymes. Furthermore, the motif of distortion can be applied to rational design of more reactive oxidative industrial catalysts, especially catalysts using transition metals such as copper.

Acknowledgments

I would like to thank my first graduate student mentor Nadia Asous, for guiding me through my first months of synthetic bioinorganic research. Dr. Wenjie Tao has also been particularly helpful in assisting me with ligand synthesis, and our conversations regarding copper-oxygen chemistry have been insightful. I could not have completed this project without financial support, which was provided by the Meyers Undergraduate Research fellowship at Ohio State. Additionally, I have greatly appreciated the support of the entire Zhang group; I always enjoy coming into the lab and I am incredibly thankful for the new friends, mentors, and colleagues I have made. Lastly, I would like to thank my fantastic faculty mentor Prof. Shiyu Zhang for always being available and providing constant support, advice, and mentorship. My research experiences in past two years and the encouragement of my colleagues have undoubtedly made me a more skillful and insightful chemist.

Supplementary Information

General experimental details

Unless otherwise noted, all experiments were carried out int a dry nitrogen atmosphere using a MBraun glovebox or through standard Schlenk technique. Unless otherwise noted solvents were dried and degassed with a Pure Process Technology (PPT) solvent purification system. Deuterated solvents were purchased from Cambridge Isotope Labs, and stored in a glovebox over 4 Å molecular sieves after degassing with N_2. Other reagents were purchased from Sigma-Aldrich, Fisher Scientific, TCI chemicals, and

Strem Chemicals. Cyclohexadiene was distilled to remove hydroquinone stabilizer. ^{1}H and ^{13}C NMR were taken on a Bruker 400 MHz and 600 MHz spectrometer, and were taken at room temperature. UV-vis spectra were taken on a Cary 60 spectrophotometer with a Unisoku Unispeks cryostat (100 to –125 °C range).

Synthesis of $^{Ph,H}BOX_{Ph,H}$ ligand

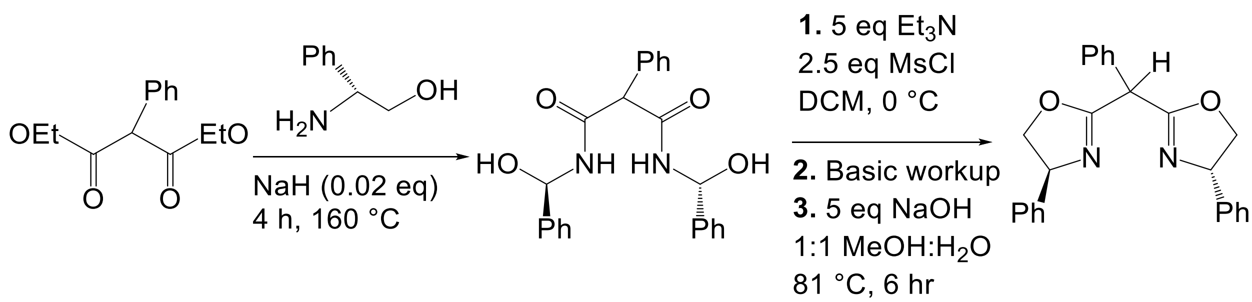

To a Schlenk flask was added diethyl phenylmalonate (3.729 mL, 0.0175 mol, 1 eq), NaH (15.7 mg, 0.02 eq), and (R)-2-phenylglycinol (4.9874 g, 0.0363 mol, 2 eq). This mixture was stirred at 130 °C under an N_2 atmosphere for 4 hr. The mixture was then vacuumed for 1 hr to remove EtOH. To the resulting oil was added dry DCM (40 mL) and Et_3N (3.879 mL, 0.0528 mol, 3 eq). After homogenizing the mixture, the solution was chilled at 0 °C and methanesulfonyl chloride (3.386 mL, 0.04375 mol, 2.5 eq) was added dropwise. Following stirring for 1 hr, the solution was worked up with saturated NH_4Cl. Solvent of the organic layer was removed in vacuo yielding a dark orange oil. The oil was dissolved in a 1:1 MeOH:H_2O mixture (60 mL) to which was added NaOH (3.4997 g, 0.0875 mol, 5 eq). The solution was refluxed at 83 °C overnight, and the precipitate was recovered via vacuum filtration and rinsed with cold water (3 x 10 mL) yielding a white powder (1.5929 g, 23.8% yield). This compound exists as a tautomer, which is evident in the NMR spectrum. ^{1}H NMR (400 MHz, Chloroform-*d*) δ 7.4-7.55 (m, 15H), 5.25 (d, 2H), 5 (s, 1H), 4.6 (m, 2H), 4.2 (m, 2H).

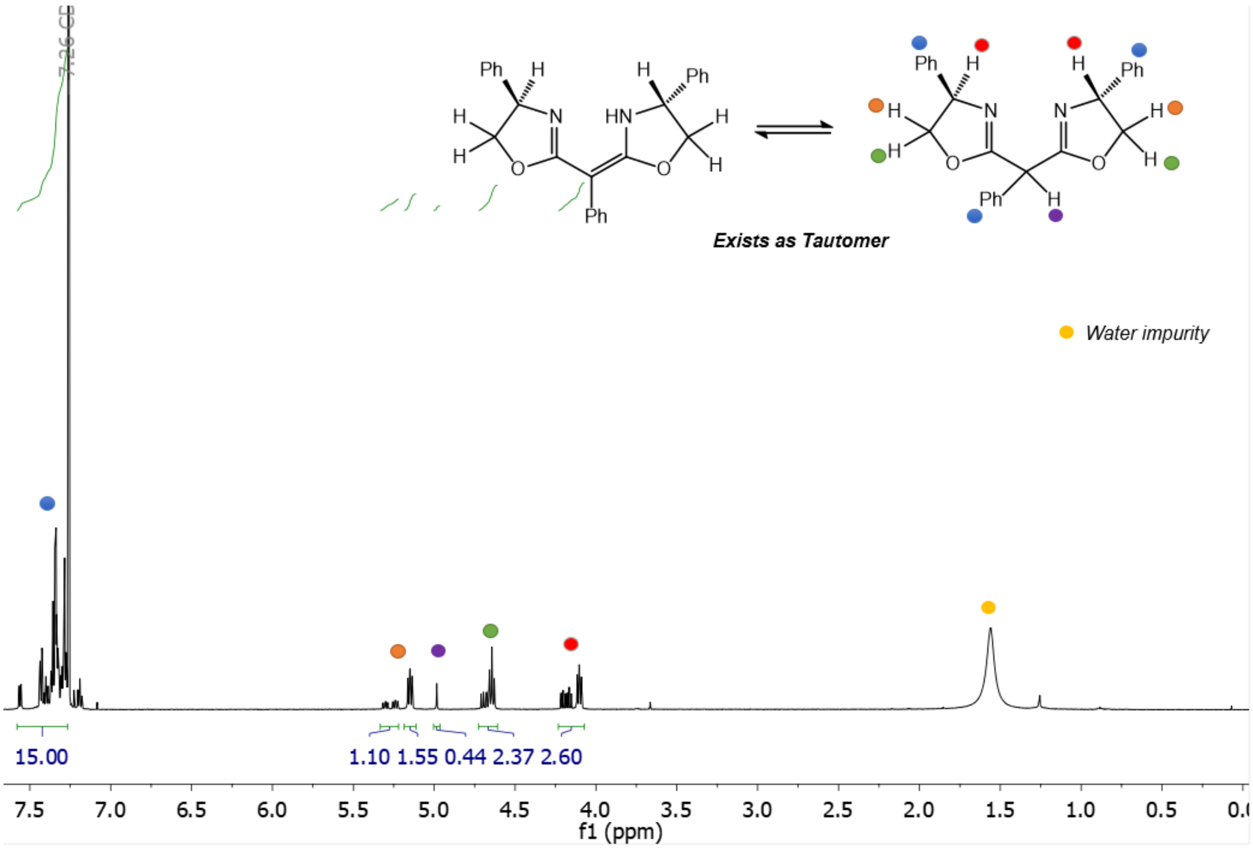

Synthesis of $^{Ph,H}BOX_{Me2}$ ligand

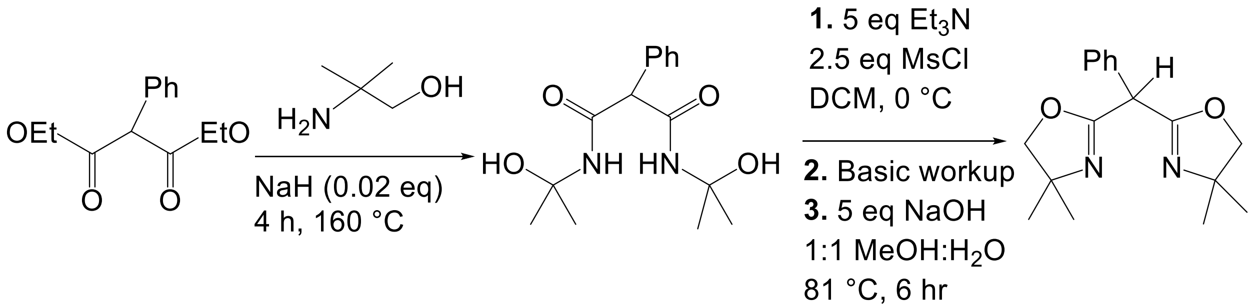

A modified procedure[18] was used to synthesize this compound. To a Schlenk flask was added diethyl phenylmalonate (2.1413 mL, 0.009924 mol, 1 eq), NaH (16.9 mg, 0.7058 mmol, 0.02 eq), and 2-amino-2-methyl-1-propanol (6.2914 g, 0.01984 mol, 2 eq). This mixture was stirred at 130 °C under an N_2 atmosphere for 3 hr. Immediately after, the mixture was vacuumed for 1 hr to remove EtOH. To the resulting oil was added dry DCM (40 mL) and Et_3N (24.6 mL, 0.176 mol, 5 eq). After homogenizing the mixture, the solution was chilled at 0 °C and methanesulfonyl chloride (6.81 mL, 0.88 mol, 2.5 eq) was added dropwise. Following stirring for 1 hr, the solution was worked up with saturated NH_4Cl. Solvent of the organic layer was removed in vacuo yielding a pale yellow oil. The oil was dissolved in a 1:1 MeOH:H_2O mixture (120 mL) to which was added NaOH (7.039 g, 0.176 mol, 5 eq). The solution was refluxed at 81 °C overnight, and the precipitate was recovered via vacuum filtration and rinsed with cold water (3 x 10 mL) yielding a white powder (3.34 g, 33% yield). This compound exists as a tautomer, which is evident in the NMR spectrum. ^{1}H NMR (400 MHz, Chloroform-*d*) δ 7.1-7.6 (m, 5H), 4.73 (s, 2H), 4-3.9 (m, 4H), 1.36 (s, 6H), 1.3 (s, 1H), 1.26 (s, 1H).

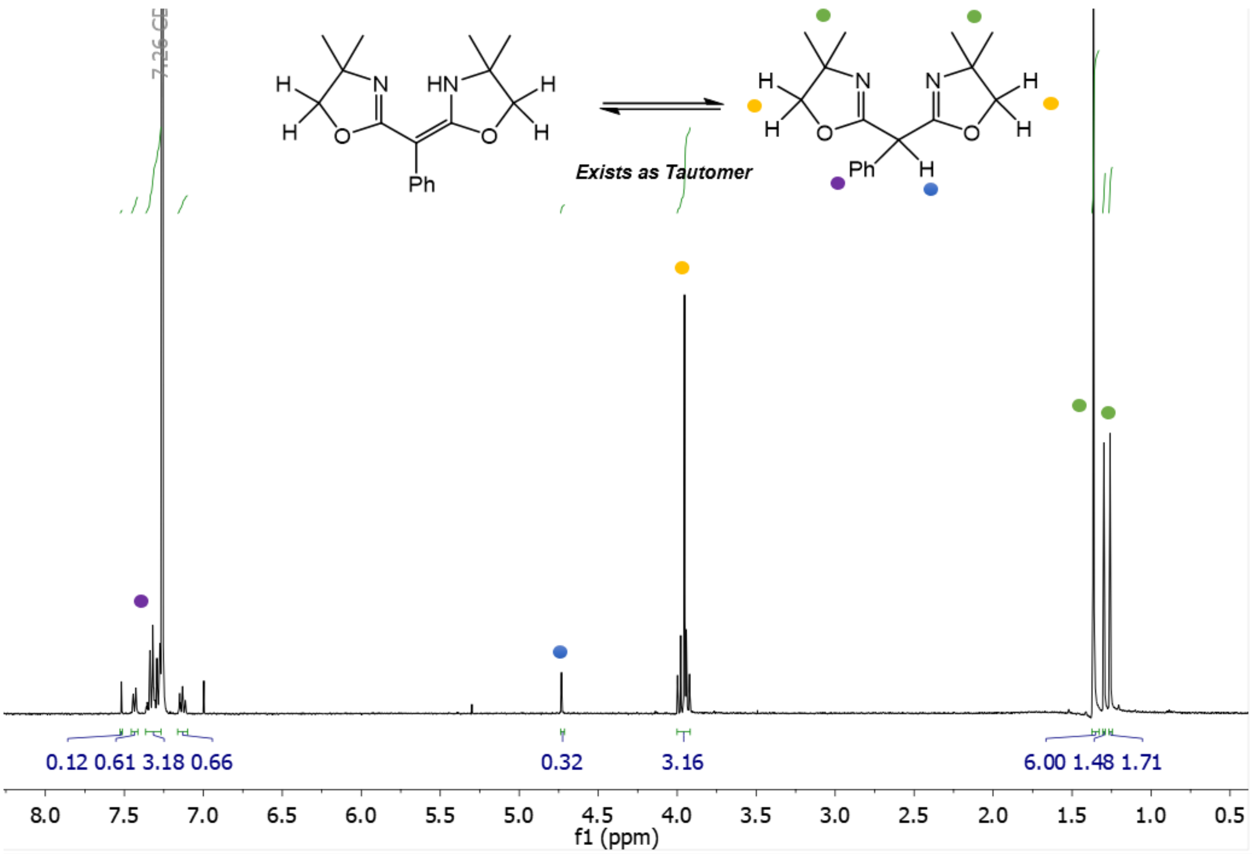

Synthesis of (^{Ph}BOX$_{Ph,H}$)Cu^{I}(MeCN)

To a stirring suspension of ^{Ph,H}BOX$_{Ph,H}$ (99.7 mg, 0.2607 mmol, 1 eq) dissolved in THF (4 mL) was added Cu^{I}OtBu (40.2 mg, 0.2941 mmol, 1.13 eq). The solution was stirred for 25 min and filtered over a celite plug. The solution was dried in vacuo affording a light tan solid, which was washed with ether (1 mL) and dried in vacuo again yielding the final product (88.8 mg, 94% yield). ^{1}H NMR (400 MHz, Benzene-d_6) δ 3.68 (q, 2H), 4.06 (t, 2H), 4.78 (q, 2), 7.21-7.85 (m, 15H).

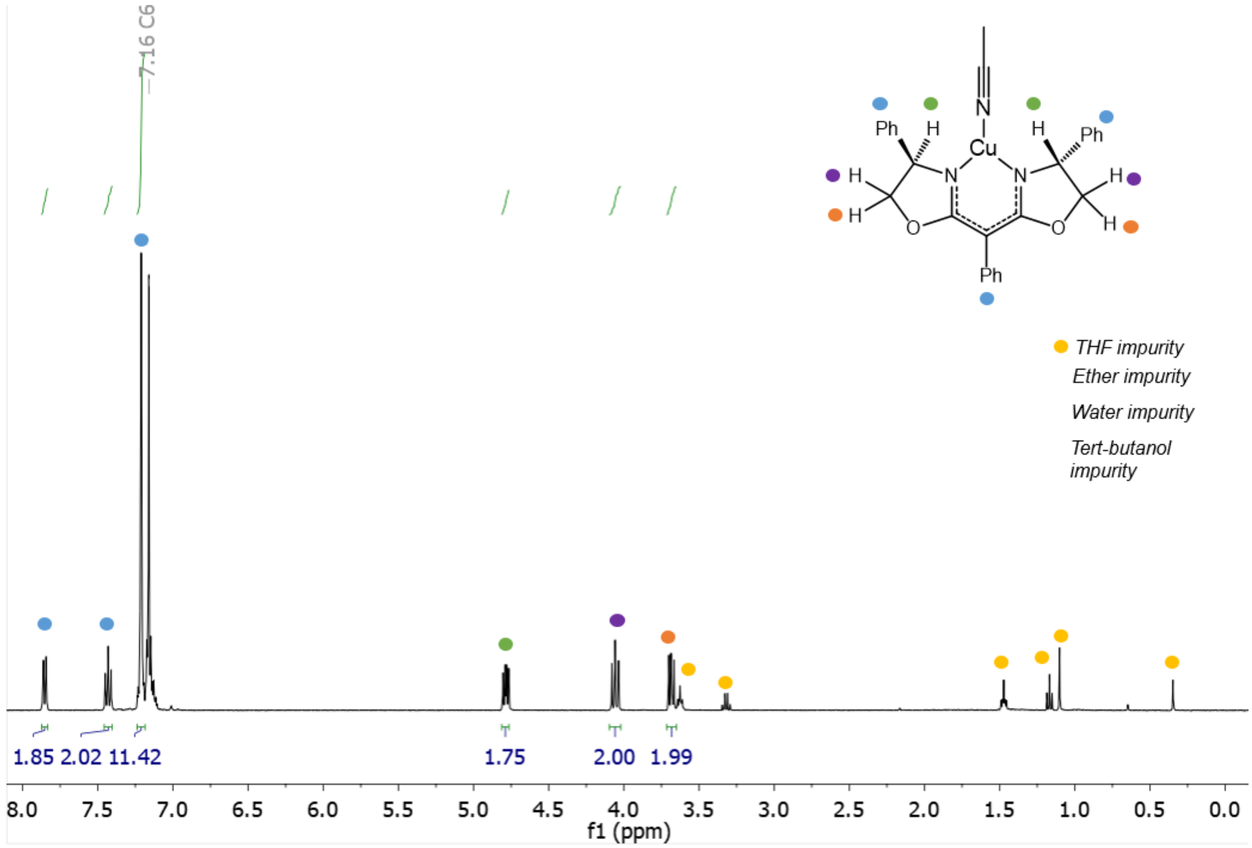

Synthesis of ($^{Ph}BOX_{Me2}$)Cu^I(MeCN)

To a suspension of $^{Ph,H}BOX_{Me2}$ (98.4 mg, 0.381 mmol, 1 eq) in THF (6 mL) was added [$Cu^I(MeCN)_4PF_6$] (145 mg, 0.381 mmol, 1 eq). This solution was stirred for 4.5 hr and filtered through a celite plug. The resulting solution was recrystallized overnight in a -35 °C freezer, and the supernatant was removed and the solid dried in vacuo. This solid was dissolved in THF (3 mL) and was cooled. To the cooled, stirring solution was added chilled LiO^tBu (61 mg, 0.762 mmol, 2 eq) dropwise. The solution was stirred for 10 min, and the solvent was removed in vacuo affording a white solid. The solid was washed with ether (3 x 1 mL) and dried in vacuo again, yielding the final product (72.2 mg, 48.8% yield). ^1H NMR (400 MHz, Benzene-d_6) δ 1.29 (s, 12H), 3.68 (s, 4H), 7.4-7.86 (m, 5H).

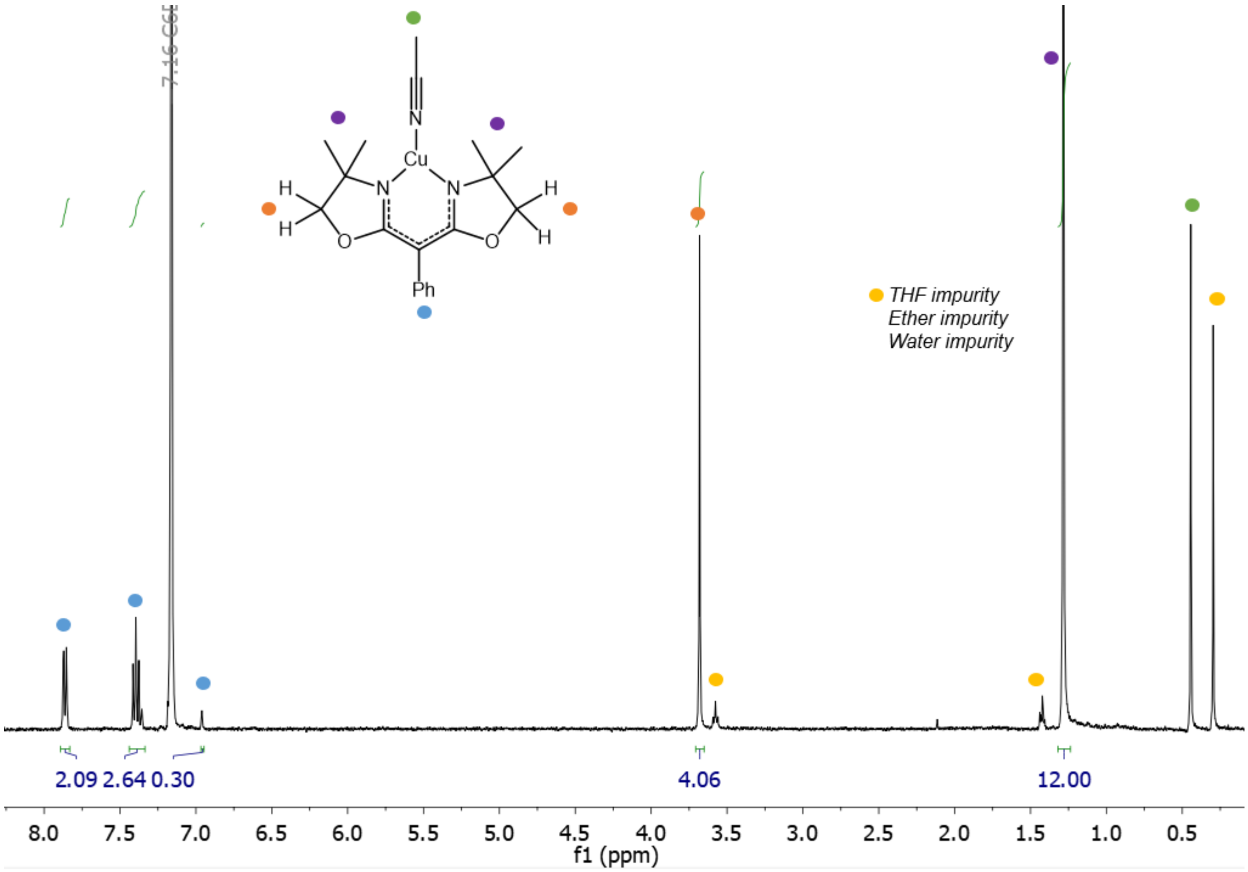

Reaction of (^{Ph}BOX$_{Ph,H}$)Cu^{I}(MeCN) with O_2

To a cuvette in a glovebox was added 0.3 mL of a 1 mM stock solution of (Ph-BOX-Ph,H)Cu^{I}(MeCN) in THF, which was subsequently diluted with 2.7 mL of THF. A septum cap was placed on the cuvette which was then removed from the glovebox and placed into the UV-vis. The temperature was set at -80 °C and a N_2 purging needle was placed through the septum cap. After allowing the solution to cool for ten minutes, dry O_2 (99.9%, excess) was bubbled through the solution via syringe, rapidly affording the **O**-Ph,H compound.

Reaction of ($^{Ph}BOX_{Me2}$)Cu^{I}(MeCN) with O_2

To a cuvette in a glovebox was added 0.3 mL of a 1 mM stock solution of [$^{Ph}BOX_{Me2}$]Cu^{I} in THF, which was subsequently diluted with 2.7 mL of THF. A septum cap was placed on the cuvette which was then removed from the glovebox and placed into the UV-vis. The temperature was set at -80 °C and a N_2 purging needle was placed through the septum cap. After allowing the solution to cool for ten minutes, dry O_2 (99.9%, excess) was bubbled through the solution via syringe, rapidly affording the **O**-Me_2 compound.

Reaction of **O**-Ph,H and **O**-Me_2 with substrates

After carrying out the oxygenation procedure, variable amounts of substrate were added. Solutions of TEMPO-H, 9,10-DHA, 1,4-cyclohexadiene, and 2,4-ditertbutyl phenol were made from commercially obtained pure solid or liquid compounds. Depending on the desired number of equivalents, different concentrations were used. The desired solution (0.1 mL) was loaded into a syringe, and was rapidly injected into the cuvette through the septum cap.

Beers law plot for (^{Ph}BOX$_{Ph,H}$)Cu^{I}(MeCN)

A beers law plot was created for the 360 nm peak of **O**-Ph,H (Figure S1). A 0.1 mM solution of (^{Ph}BOX$_{Ph,H}$)Cu^{I}(MeCN) (2 mL) was added to a cuvette and 5 additions of 0.2 mL of cold THF were added.

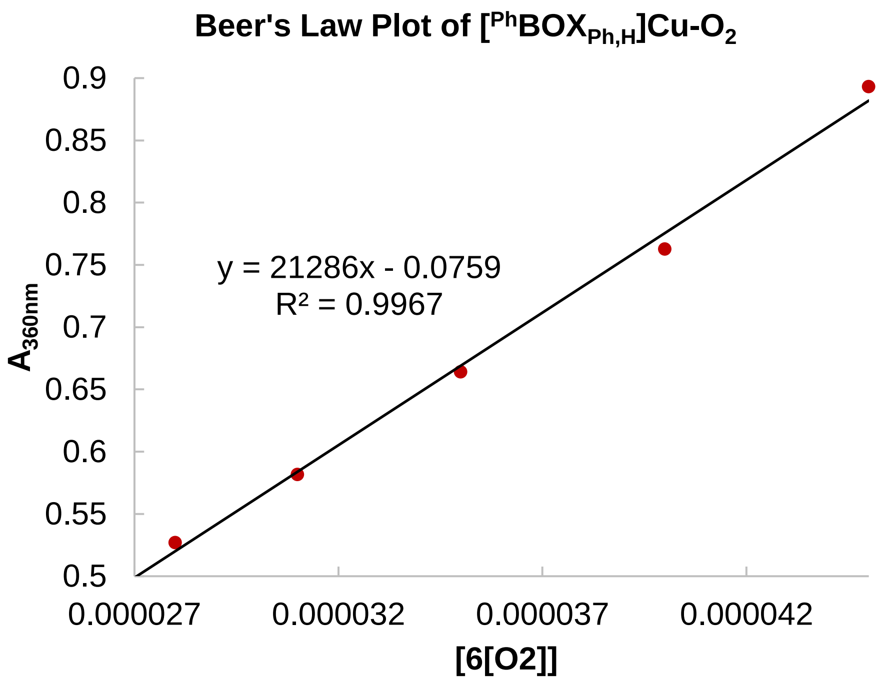

Figure S1. Beers law plot of the 360 nm peak of **O**-Ph,H.

Beers Law plot of [$^{Ph}BOX_{Me2}$]Cu with O_2

A Beers Law plot was created for the 337 nm peak of **O**-Me_2. A 0.5 mM solution (2 mL) was added to a cuvette and five additions of 0.2 mL of cold THF were added. The molar absorptivity was determined to be 6,308 $M^{-1}cm^{-1}$.

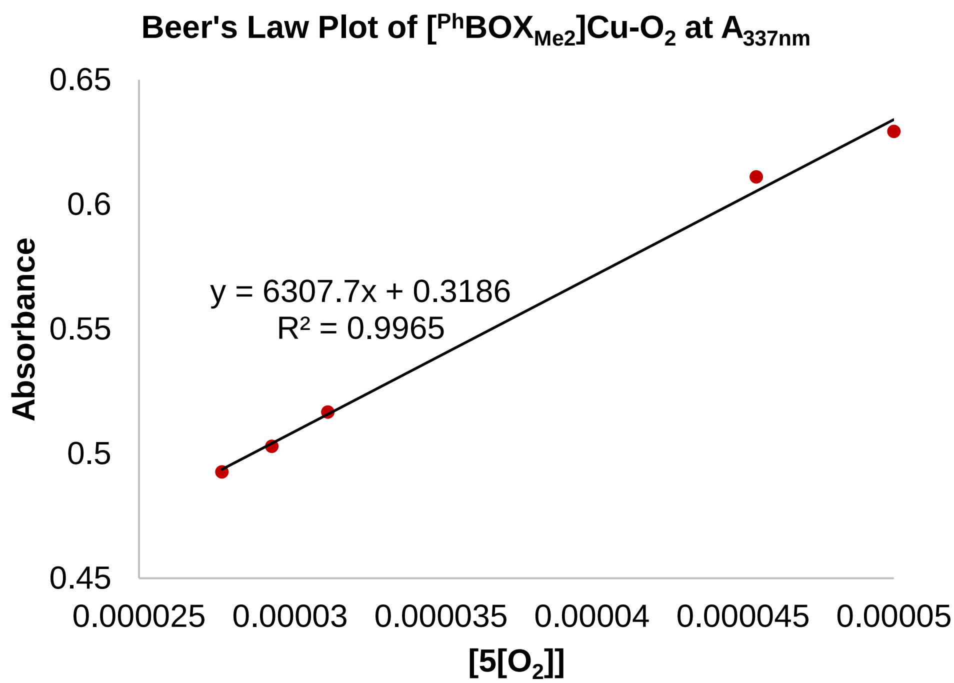

Figure S2. Beers law plot of the 337 nm peak of **O**-Me_2.

EPR Reaction of **O**-Ph,H + 100 eq of 2,4-ditertbutylphenol

Outside of the glovebox, to an EPR tube was added 0.2 mL of [$^{Ph}BOX_{Ph,H}$]Cu^{I}(MeCN) (0.1 mM). This solution was chilled at -80 °C for ten minutes, and oxygen was added. After ten minutes, the solution was treated with 100 equivalents of 2,4-ditertbutylphenol (0.1 mL). This solution was allowed to react for 2 hours while maintaining temperature at -80 °C. The sample was then frozen in liquid N_2, and the EPR spectrum was taken. It was taken at 20K, and the final concentration of Cu was 0.1 mM. No hyperfine features were observed. The following parameters were used 9.64 GHz, 20K; parameters g|| = 2.210, g (perpendicular) = 2.054. A|| = 185 * 10E-4. A (perp.) = 14N 10E-4 cm.

Synthesis of $^{Ph,H}BOX_{H,H}$

This compound was provided by Dr. Wenjie Tao.

Synthesis of $^{Ph,H}BOX_{Me,H}$

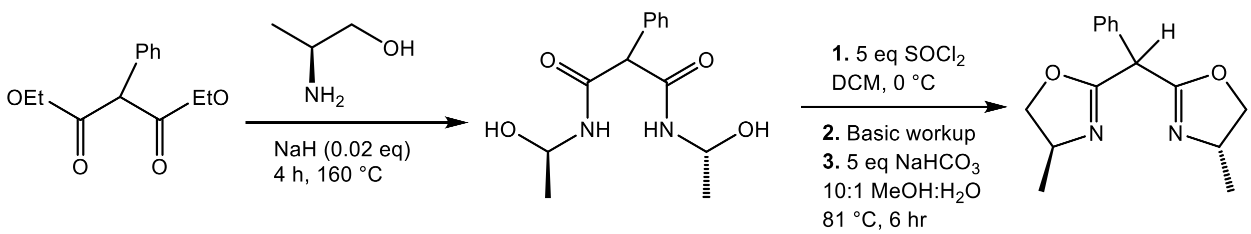

A stirred mixture of the diethyl phenylmalonate (2 mL, 2.19 g, 9.269 mmol, 1 eq) with 2.00 eq (S)-2-aminopropanol (L-alaninol) (1.44 mL, 1.39 g, 18.54 mmol, 2 eq) and 0.02 eq sodium hydride (4.45 mg, 0.18538 mmol, 0.02 eq) was heated in an Ace Glass heavy-wall pressure tube under a nitrogen atmosphere to 130 °C for 3 hours. Ethanol was then removed under vacuum when it was still hot for 1 hr. The solid compound was dissolved in a solution of dry toluene (40 mL) and DCM (20 mL). $SOCl_2$ (5 mL, 70 mmol, 5 eq) was added dropwise and stirred for 3 hours at 70 °C. The amber solution was worked up with saturated sodium bicarbonate, and the organic layer was collected and dried with Na_2SO_4. Solvent was removed in vacuo, and the product was redissolved in MeOH (60 mL) and H_2O (6 mL) and refluxed at 80 °C for 12 hrs. MeOH was removed in vacuo and the product was extracted from the organic layer after adding additional H_2O (20 mL) and

DCM (2 x 30 mL). DCM was removed in vacuo to yield a waxy solid (1.812 g, yield = 50.4%). This compound also exists as a tautomer, and two forms are present as evidenced by the NMR spectrum. ^{1}H NMR (400 MHz, $CDCl_3$) δ 7.25-7.5 (m, 5H), 4.75 (s, 1H), 4.4 (m, 2H), 4.3 (m, 2H), 3.8 (m, 2H), 1.3 (m, 6H).

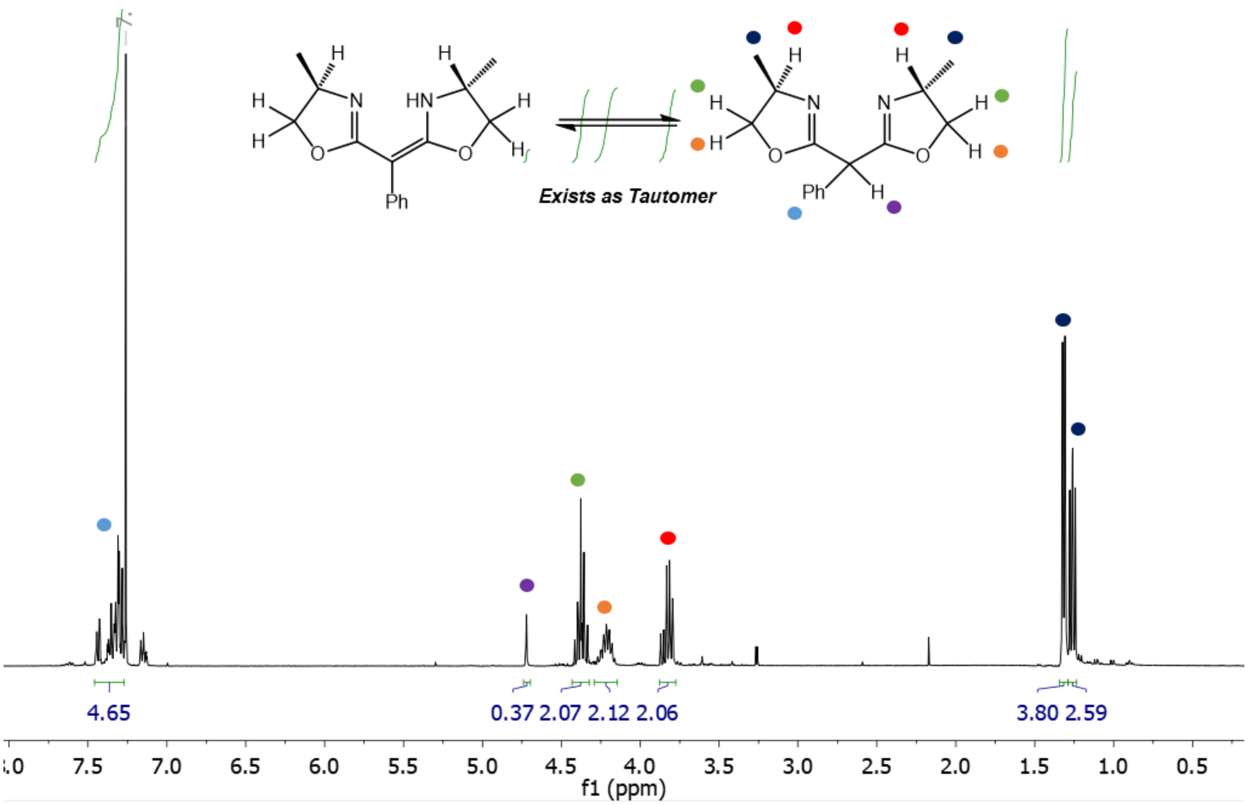

In-situ reaction to form $[(^{Ph,H}BOX_{Me,H})_2Cu_2O_2]^{2+}$

$[Cu(MeCN)_4]CF_3SO_3$ (6.7 mg, 0.018 mmol, 1 eq) was dissolved in THF (2 mL) in a cuvette. The cuvette was placed in the UV-vis and was cooled at -40 °C for 10 min. $^{Ph,H}BOX_{Me,H}$ (4.56 mg, 0.018 mmol, 1 eq) was dissolved in THF (1 mL) and added dropwise to the cuvette with stirring at -40 °C. The solution was allowed to react for 50 minutes at -40 °C, and O_2 was added.

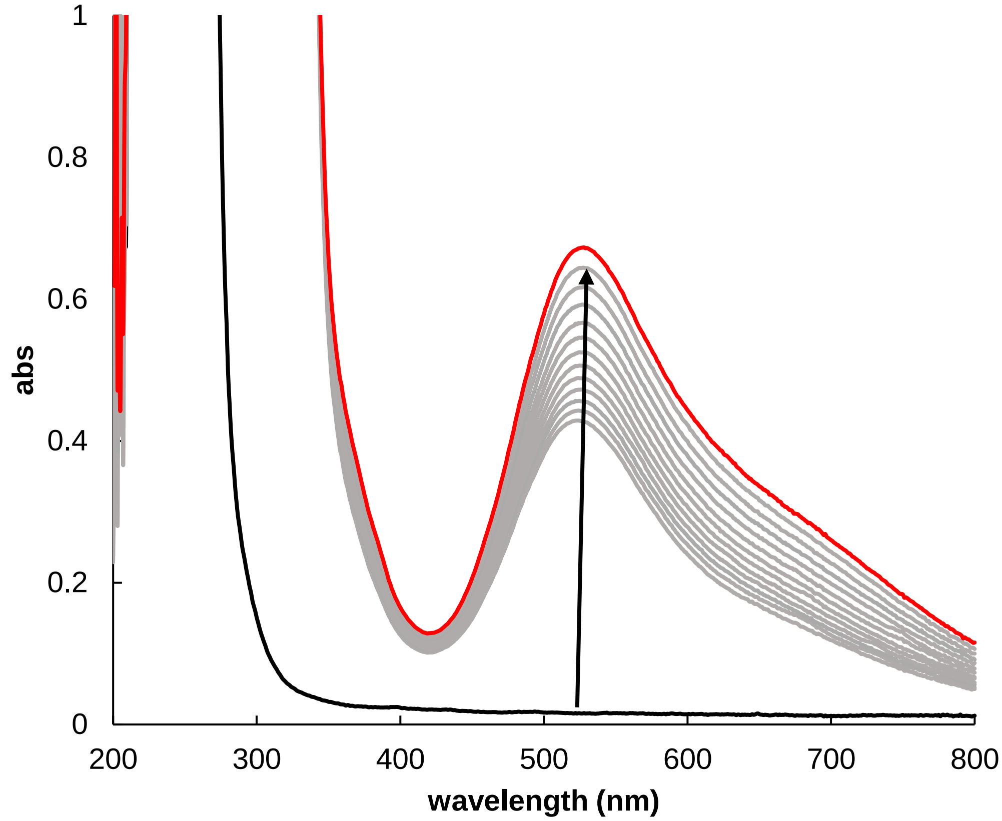

Figure S3. UV-Vis spectrum of $[Cu^{I}(MeCN)_4]CF_3SO_3$ (-40 °C, 3 mM, THF) treated with 1 equiv of $^{Ph}BOX_{Me,H}$. Addition of O_2 does not change the spectrum features.

In-situ reaction to form $[(^{Ph,H}BOX_{H,H})_2Cu_2O_2]^{2+}$

$[Cu^{I}(MeCN)_4]CF_3SO_3$ (6.7 mg, 0.018 mmol, 1.1 eq) was dissolved in THF (2 mL) in a cuvette. The cuvette was placed in the UV-vis and was cooled at -40 °C for 10 min. $^{Ph,H}BOX_{H,H}$ (4.56 mg, 0.020 mmol, 1.11 eq) was dissolved in THF (1 mL) and added dropwise to the cuvette with stirring at -40 °C. The solution was allowed to react for 50 minutes at -40 °C, and O_2 was added.

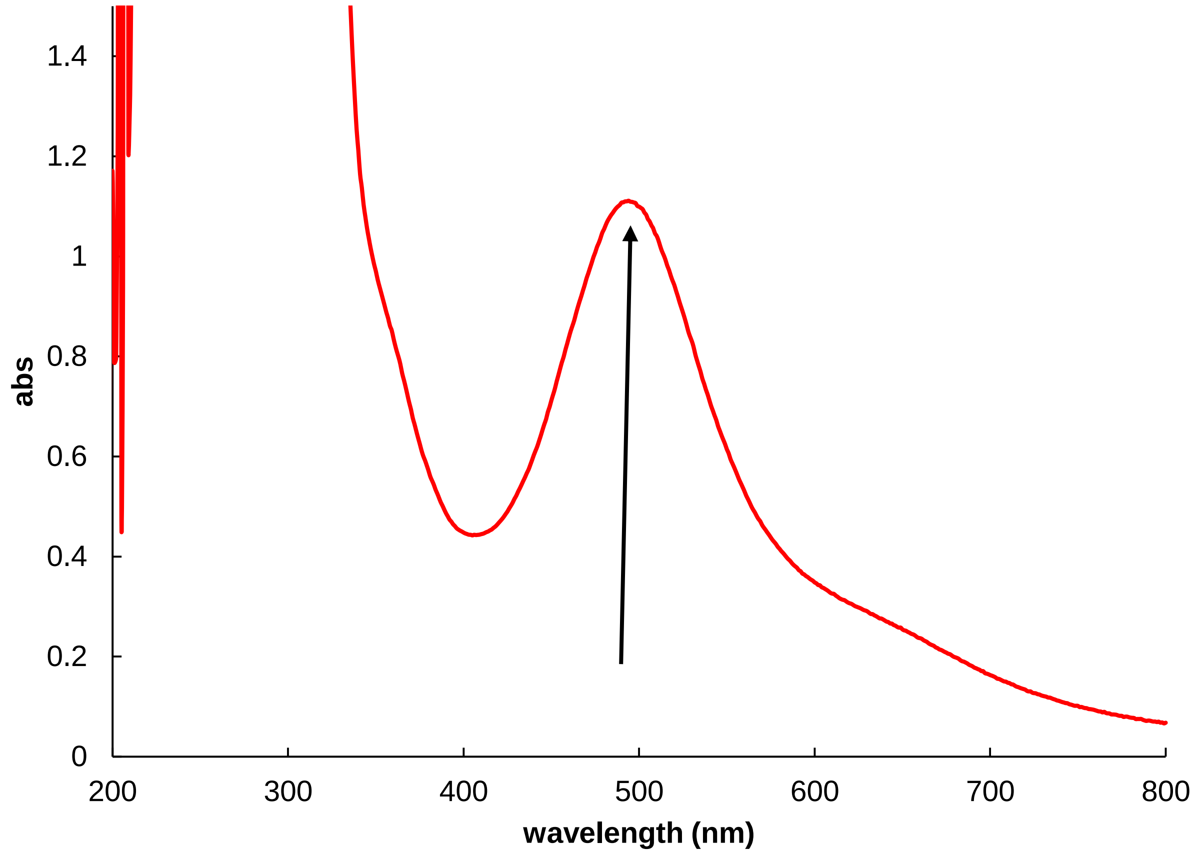

Figure S4. UV-Vis spectrum of $[Cu^{I}(MeCN)_4]CF_3SO_3$ (-40 °C, 3 mM $[Cu_2]$, THF) treated with 1 equiv of $^{Ph}BOX_{H,H}$. Addition of O_2 does not change the spectrum features.

"Core Capture" method attempted synthesis of $[(^{Ph}BOX_{H,H})_2Cu_2O_2]$

This procedure is adapted from Stack and coworkers[16]. In order to create a more anionic ligand, $^{Ph,H}BOX_{H,H}$ was first deprotonated with the following method. To a stirring solution of $^{Ph,H}BOX_{H,H}$ (43.7 mg in 1 mL of THF) was added KO^{t}Bu (22.4 mg in 1 mL of THF, 1 eq). After the addition, a white cloudy mixture was formed. THF (3 mL) was added to try to dissolve the cloudy solid, but it was still cloudy. This probably indicates the organic salt was immediately formed. This suspension was stirred for 4 hours, then solvent was removed in vacuo. An NMR in acetone-d_6 was taken to confirm the deprotonation was successful. A solution of $Cu^I(MeCN)_4CF_3SO_3$ (0.0720 mL of a 2.5 mM solution) was added to a cuvette of THF (2.428 mL) which was chilled in the UV-Vis at -80 °C for 10 min. To this was added N,N,N′,N′-tetramethyl-1,3-propanediamine (abbreviated TMPD, 0.1 mL of a 1.801 mM solution). Excess O_2 was then immediately injected via syringe, forming the 400 nm peak corresponding to the $(TMPD)_2[Cu_2O_2]^{2+}$ bis(μ-oxo) core observed in the literature (final concentration = 0.033 mM). After 5 min, a solution of $^{Ph}BOX_{H,H}$ (0.1 mL of a 1.8009 mM) solution was added via syringe. The 400 nm peak decreased greater than it would if it was only diluted, indicating the added $^{Ph}BOX_{H,H}$ ligand disrupted the pre-formed core in some manner. Subsequently, a small 500 nm peak began to grow, likely corresponding to the tetrahedral $[(^{Ph}BOX_{H,H})_2Cu^{II}]$ product.

“Core Capture” method attempted synthesis of $[(^{Ph}BOX_{Me,H})Cu_2O_2]$

This procedure is adapted from Stack and coworkers[16]. In order to create a more anionic ligand, $^{Ph,H}BOX_{Me,H}$ was first deprotonated with the following method. To a stirring solution of $^{Ph,H}BOX_{Me,H}$ (69.1 mg in 2 mL of THF) was added KO^tBu (22.4 mg in 1 mL of THF, 1 eq). After the addition, a white cloudy mixture was formed. This suspension was stirred for 2 hours, then solvent was removed in vacuo. An NMR in acetone-d_6 was taken to confirm the deprotonation was successful. A solution of $Cu^I(MeCN)_4CF_3SO_3$ (2.5 mL of a 10 mM solution) was added to a cuvette, which was chilled in the UV-Vis at -80 °C for 10 min. To this was added N,N,N′,N′-tetramethyl-1,3-propanediamine (abbreviated TMPD, 0.5 mL of a 49.98 mM solution). Excess O_2 was then immediately injected via syringe, forming the 400 nm peak corresponding to the $(TMPD)_2[Cu_2O_2]^{2+}$ bis(μ-oxo) core observed in the literature (final concentration = 4.16 mM). After 5 min, a solution of $[^{Ph}BOX_{H,H}]K$ (0.5 mL of a 58.31 mM) solution was added via syringe. The 400 nm peak immediately began to decay with subsequent growth of a peak a 520 nm. This 520 nm peak was previously attributed to the tetrahedral $[(^{Ph,H}BOX_{H,H})_2Cu^{II}]^{2+}$ product.

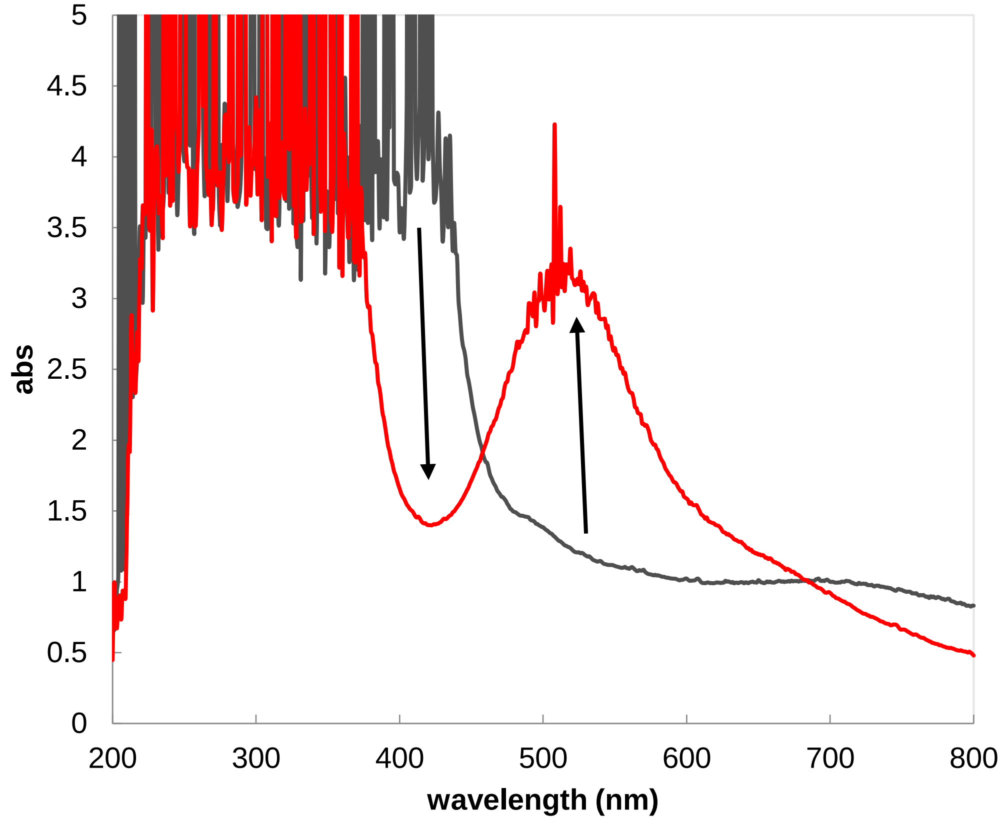

Figure S5. UV-Vis spectrum of $[(TMPD)_2Cu_2O_2]$ (-80 °C, 4.16 mM $[Cu_2]$, THF) treated with 1 equiv of $^{Ph}BOX_{H,H}$..

References

(1) Faramawy, S.; Zaki, T.; Sakr, A. A. E. Natural Gas Origin, Composition, and Processing: A Review. *Journal of Natural Gas Science and Engineering*. Elsevier B.V. August 1, 2016, pp 34–54. https://doi.org/10.1016/j.jngse.2016.06.030.

(2) Comprehensive Handbook of Chemical Bond Energies - Yu-Ran Luo (CRC, 2007).Pdf.

(3) Olivos-Suarez, A. I.; Szécsényi, À.; Hensen, E. J. M.; Ruiz-Martinez, J.; Pidko, E. A.; Gascon, J. Strategies for the Direct Catalytic Valorization of Methane Using Heterogeneous Catalysis: Challenges and Opportunities. *ACS Catal.* **2016**, *6* (5), 2965–2981. https://doi.org/10.1021/acscatal.6b00428.

(4) Balasubramanian, R.; Smith, S. M.; Rawat, S.; Yatsunyk, L. A.; Stemmler, T. L.; Rosenzweig, A. C. Oxidation of Methane by a Biological Dicopper Centre. *Nature* **2010**, *465* (7294), 115–119. https://doi.org/10.1038/nature08992.

(5) Culpepper, M. A.; Cutsail, G. E.; Gunderson, W. A.; Hoffman, B. M.; Rosenzweig, A. C. Identification of the Valence and Coordination Environment of the Particulate Methane Monooxygenase Copper Centers by Advanced EPR Characterization. *J. Am. Chem. Soc.* **2014**, *136* (33), 11767–11775. https://doi.org/10.1021/ja5053126.

(6) Culpepper, M. A.; Cutsail, G. E.; Hoffman, B. M.; Rosenzweig, A. C. Evidence for Oxygen Binding at the Active Site of Particulate Methane Monooxygenase. *J. Am. Chem. Soc.* **2012**, *134* (18), 7640–7643. https://doi.org/10.1021/ja302195p.

(7) Cao, L.; Caldararu, O.; Rosenzweig, A. C.; Ryde, U. Quantum Refinement Does Not Support Dinuclear Copper Sites in Crystal Structures of Particulate Methane Monooxygenase. *Angew. Chemie - Int. Ed.* **2018**, *57* (1), 162–166.

https://doi.org/10.1002/anie.201708977.

(8) Ross, M. O.; MacMillan, F.; Wang, J.; Nisthal, A.; Lawton, T. J.; Olafson, B. D.; Mayo, S. L.; Rosenzweig, A. C.; Hoffman, B. M. Particulate Methane Monooxygenase Contains Only Mononuclear Copper Centers. *Science.* **2019**, *364* (6440), 566–570. https://doi.org/10.1126/science.aav2572.

(9) Elwell, C. E.; Gagnon, N. L.; Neisen, B. D.; Dhar, D.; Spaeth, A. D.; Yee, G. M.; Tolman, W. B. Copper-Oxygen Complexes Revisited: Structures, Spectroscopy, and Reactivity. *Chem. Rev*. **2017**, *117* (3), 2059–2107. https://doi.org/10.1021/acs.chemrev.6b00636.

(10) Matoba, Y.; Kihara, S.; Bando, N.; Yoshitsu, H.; Sakaguchi, M.; Kayama, K.; Yanagisawa, S.; Ogura, T.; Sugiyama, M. Catalytic Mechanism of the Tyrosinase Reaction toward the Tyr 98 Residue in the Caddie Protein. *PLoS Biol.* **2018**, *16* (12). https://doi.org/10.1371/journal.pbio.3000077.

(11) Molitor, C.; Mauracher, S. G.; Rompel, A. Aurone Synthase Is a Catechol Oxidase with Hydroxylase Activity and Provides Insights into the Mechanism of Plant Polyphenol Oxidases. *Proc. Natl. Acad. Sci. U. S. A.* **2016**, *113* (13), E1806-15. https://doi.org/10.1073/pnas.1523575113.

(12) Matoba, Y.; Kumagai, T.; Yamamoto, A.; Yoshitsu, H.; Sugiyama, M. Crystallographic Evidence That the Dinuclear Copper Center of Tyrosinase Is Flexible during Catalysis. *J. Biol. Chem.* **2006**, *281* (13), 8981–8990. https://doi.org/10.1074/jbc.M509785200.

(13) Goswami, V. E.; Walli, A.; Förster, M.; Dechert, S.; Demeshko, S.; Holthausen, M. C.; Meyer, F. Acid/Base Triggered Interconversion of μ-η^2: η^2-Peroxido and Bis(μ-

Oxido) Dicopper Intermediates Capped by Proton-Responsive Ligands. *Chem. Sci.* **2017**, *8* (4), 3031–3037. https://doi.org/10.1039/c6sc04820j.

(14) Pidcock, E.; Obias, H. V; Abe, M.; Liang, H.-C.; Karlin, K. D.; Solomon, E. I. Spectroscopic and Theoretical Studies of Oxygenated Dicopper(I) Complexes Containing Hydrocarbon-Linked Bis[2-(2-Pyridyl)Ethyl]Amine Units: Investigation of a Butterfly $[Cu_2 (\mu\text{-}\eta^2:\eta^2)(O_2)]^{2+}$ Core. J. Am. Chem. Soc. **1999,** *121* (6), 1299-1308. https://doi.org/10.1021/ja983310e.

(15) Funahashi, Y.; Nishikawa, T.; Wasada-Tsutsui, Y.; Kajita, Y.; Yamaguchi, S.; Arii, H.; Ozawa, T.; Jitsukawa, K.; Tosha, T.; Hirota, S.; et al. Formation of a Bridged Butterfly-Type μ-H2: H2-Peroxo Dicopper Core Structure with a Carboxylate Group. *J. Am. Chem. Soc.* **2008**, *130* (49), 16444–16445. https://doi.org/10.1021/ja804201z.

(16) Citek, C.; Lin, B. L.; Phelps, T. E.; Wasinger, E. C.; Stack, T. D. P. Primary Amine Stabilization of a Dicopper(III) Bis(μ-Oxo) Species: Modeling the Ligation in PMMO. *J. Am. Chem. Soc.* **2014**, *136* (41), 14405–14408. https://doi.org/10.1021/ja508630d.

(17) Citek, C.; Gary, J. B.; Wasinger, E. C.; Stack, T. D. P. Chemical Plausibility of Cu(III) with Biological Ligation in PMMO. *J. Am. Chem. Soc.* **2015**, *137* (22), 6991–6994. https://doi.org/10.1021/jacs.5b02157.

(18) Walli, A.; Dechert, S.; Meyer, F. Tautomerism in Bis(Oxazoline)S. *European J. Org. Chem.* **2013**, *31*, 7044–7049. https://doi.org/10.1002/ejoc.201301282.